Universidade de Aveiro Departamento de Electrónica e Telecomunicações
2007

Dorabella Martins da Silva Santos

Reconstrução de sinal em estruturas com dois canais

Signal reconstruction in structures with two channels

Universidade de Aveiro Departamento de Electrónica e Telecomunicações
2007

Dorabella Martins da Silva Santos

Reconstrução de sinal em estruturas com dois canais

Signal reconstruction in structures with two channels

DOCUMENTO PROVISÓRIO

Universidade de Aveiro Departamento de Electrónica e Telecominicações
2007

Dorabella Martins da Silva Santos

Reconstrução de sinal em estruturas com dois canais

Signal reconstruction in structures with two channels

Dissertação apresentada à Universidade de Aveiro para cumprimento dos requisitos necessários à obtenção do grau de Doutor em Engenharia Electrotécnica, realizada sob a orientação científica do Prof. Dr. Paulo Jorge dos Santos Gonçalves Ferreira, Professor Catedrático do Departamento de Electrónica e Telecomunicações da Universidade de Aveiro e co-orientação científica do Prof. Dr. José Manuel Neto Vieira, Professor Auxiliar do Departamento de Electrónica e Telecomunicações da Universidade de Aveiro.

Apoio financeiro do POCTI no âmbito
do III Quadro Comunitário de Apoio.

o júri

presidente — Reitora da Universidade de Aveiro

Doutor Paulo Jorge dos Santos Gonçalves Ferreira
professor catedrático da Universidade de Aveiro

Doutor Jorge dos Santos Salvador Marques
professor associado do Instituto Superior Técnico da Universidade Técnica de Lisboa

Doutor Vítor Manuel Mendes da Silva
professor auxiliar da Faculdade de Ciências e Tecnologia da Universidade de Coimbra

Doutor Aníbal João de Sousa Ferreira
professor auxiliar da Faculdade de Engenharia da Universidade do Porto

Doutor José Manuel Neto Vieira
professor auxiliar da Universidade de Aveiro

agradecimentos

Quero agradecer aos meus orientadores pela excelente disposição e amizade e pela orientação preciosa, sem a qual esta tese não poderia ter sido elaborada; a todos os colegas de trabalho pelo ambiente acolhedor e pela sua amizade; e à minha família que me tem apoiado ao longo deste percurso.

palavras-chave

Detecção e correcção de erros, algoritmos de reconstrução, estabilidade numérica, interpolação.

resumo

Em sistemas ATM e transmissões em tempo real através de redes IP, os dados são transmitidos em pacotes de informação. Os pacotes perdidos ou muito atrasados levam à perda de informação em posições conhecidas (apagamentos). Contudo, em algumas situações as posições dos erros não são conhecidas e, portanto, a detecção dos erros tem que ser realizada usando um polinómio conhecido.

A detecção e correcção de erros são estudadas para sinais digitais em códigos DFT em dois canais que apresentam muito melhor estabilidade que os respectivos códigos DFT num único canal. Para a estrutura de dois canais, um canal processa um código DFT normal, quanto que o outro canal inclui uma permutação, a razão principal para a melhoria na estabilidade. A permutação introduz aleatoriedade e é esta aleatoriedade que é responsável pela boa estabilidade destes códigos. O estudo dos códigos aleatórios vêm confirmar esta afirmação.

Para sinais analógicos, foca-se a amostragem funcional e derivativa, onde um canal processa amostras do sinal e o outro processa amostras da derivada do sinal. A expansão sobreamostrada é apresentada e a recuperação de apagamentos é estudada. Neste caso, a estabilidade para a esturtura em dois canais quando a perda de amostras afecta ambos os canais é, em geral, muito pobre.

Adicionalmente, a reconstrução de sinais tanto analógicos como digitais é tratada para o modelo do conversor *integrate-and-fire*. A reconstrução faz uso dos tempos de acção e de valores limites inerentes ao modelo e é viável por meio de um método iterativo baseado em projecções em conjuntos convexos (POCS).

keywords Error detection and correction, reconstruction algorithms, numerical stability, interpolation.

abstract

In ATM as in real time transmissions over IP networks, the data are transmitted packet by packet. Lost or highly delayed packets lead to lost information in known locations (erasures). However, in some situations the error locations are not known and, therefore, error detection must be performed using a known polynomial.

Error detection and correction are studied for digital signals in two-channel DFT codes which presents a much better stability than their single channel counterparts. For the two-channel structure, one channel processes an ordinary DFT code, while the other channel includes an interleaver, the main reason for the improvement in stability. The interleaver introduces randomness and it is this randomness that is responsible for the good stability of these codes. The study of random codes helps confirm this statement.

For analogical signals, the focus is given to function and derivative sampling, where one channel processes samples of the signal and the other processes samples of the derivative of the signal. The oversampled expansion is presented and erasure recovery is studied. In this case, the stability of the two-channel structure when sample loss affects both channels is, in general, very poor.

Additionally, the reconstruction of analogical as well as digital signals is dealt with for the integrate-and-fire converter model. The reconstruction makes use of the firing times and the threshold values inherent to the model and is viable by means of an iterative method based on projections onto convex sets (POCS).

Contents

Chapter 1

Introduction

1.1 Overview

The main subject of this thesis is signal (or symbol) reconstruction, which has been studied in a number of different contexts. This thesis consists of six chapters: the introduction; the study of the role of randomness in the stability of real-number block codes, giving a comparison between DFT, PCC and random codes (the codes in this chapter deal with a finite number of samples of a discrete time signal); the study of the recovery of missing samples in oversampled filter banks, especially for the function and derivative filter bank (in this chapter an infinite number of samples of a continuous time signal is considered); the discovery of a certain pattern of redundancy in DNA sequences that can be equated by a special polynomial which also occurs in error-location; the study of reconstruction for the integrate-and-fire converter; and a chapter harboring the conclusions. Although the four main chapters are independent from each other, a common denominator can be found: redundancy and reconstruction. Nevertheless, these issues are studied in very different contexts and are treated very differently in each of the main chapters, since the nature of the problems studied there is distinct.

1.1.1 Real-Number Codes

This chapter focuses on erasure channels, which occur in many problems. For example, in ATM systems as in real time transmission over IP networks, the data are transmitted packet by packet. The packets are routed independently of each other and reassembled at

the receiver. Such packet transmission systems are prone to losses. Lost or highly delayed packets lead to errors at known locations known as erasures (missing packets).

But in many practical situations the locations of the errors may not be known. Hence error detection must be performed. The error locations can be determined by the well-known error-locating polynomial [19, 46]. This is a nonlinear problem since the locations are determined by the roots of the polynomial. Once the errors are detected, i.e., the locations are known, the problem is reduced to erasure correction which, in turn, is a linear problem.

Erasure correction, in turn, deals with the reconstruction of lost data from the received samples. This is usually done using conventional error-control coding (over finite fields), but can also be achieved by using joint source-channel codes over the real field. In fact, for applications where floating point operations are inherent, error-correction codes over finite fields may not be the best solution or may not exist at all. Instead, codes defined over the real or complex field have to be used to detect and correct errors, by taking advantage of relationships which exist only in the real or complex field, and not in finite fields.

From the frame theory perspective, overcomplete frame expansions represent such codes [37]. In this context, DFT codes which are discussed in Chapter 2 can be employed [21, 35, 45]. They have the advantage of being implementable using standard digital signal processors, not being restricted to certain block lengths and can simultaneously correct errors and reduce data rate [43]. They have been applied to the problem of algorithm-based fault tolerant designs, which are real by nature. An important result due to Nair and Abraham [32] states that for every t-error detecting code defined over the finite field, there exists a corresponding real-number code with error detectability $\geq t$. However, these codes are sensitive to background noise and are not stable under bursty losses.

The applicability of DFT codes as block codes in practice assume, however, that the transmission or storage channel is sufficiently error free or has an inner code (conventional error-control code) for correction of random errors [29]. Thus the DFT code serves as an outer code as depicted in Figure 1.1. Such a structure provides additional error-correcting capabilities without the need to modify the inner code and maintains the bit rate. The

redundancy is introduced or explored at the real field level (instead of the finite field level), increasing at the same time its compatibility, since DFT codes can be implemented as outer codes by the user with digital signal processors at the terminal points of the system.

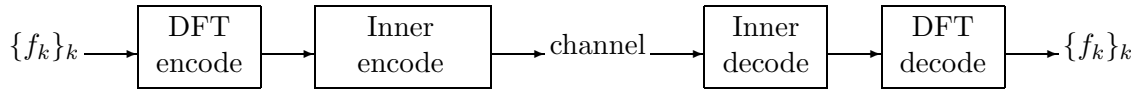

Figure 1.1: The DFT code as an outer block code. The inner code is usually a finite-field error-control code adapted to the channel.

The poor stability of DFT codes in the presence of bursty losses can be overcome if the codes are implemented in a parallel concatenated fashion (which can also be applied to the outer code scheme). Such a structure consists of two channels, where one channel employs a DFT code and the other uses additionally an interleaver. It is remarkable to note that the two-channel codes are far more stable than their single channel counterparts [22, 47]. In fact, the numerical stability of the first can be by several orders of magnitude lower (better) than the latter. Surprisingly though, a mathematical demonstration of how the interleaver intervenes has been difficult to establish, although many are the numerical results that confirm the good stability of the two-channel codes even around contiguous erasures. This can be thought intuitively to be the consequence of the permutation scattering of contiguous erasure patterns. Many studies about cycles and fixed points of permutations have been performed, but to present with little apparent relevance to explain such improvement. Actually, [22] shows that the form of the permutation is not really critical, this is, the great majority of permutations yields good condition numbers. As long as there is some level of randomness, the stability will be good. This is confirmed by the random gaussian codes [9, 48], whose performance is exceptionally stable. Although the matrices involved have no specific structure, it is possible to use these codes to detect errors. This is a combinatorial problem by nature, but under certain sparsity conditions the combinatorics can be circumvented [13, 14, 15, 28].

1.1.2 Oversampled Filter Banks

Reconstruction of lost data implies redundancy and, therefore, oversampled sampling expansions may additionally be used to obtain the original bandlimited signal [30]. If the system is critically sampled (sampled at exactly the Nyquist rate), then the loss of data yields reconstruction impossible. Yet oversampling (sampling at a rate higher that the critical rate) allows exact reconstruction for the classical sampling setup (one channel case) when any finite number of samples is lost [16, 17, 31]. Moreover, it is well known that if a signal is undersampled (sampled at a rate lower than the critical one) the signal cannot even be reconstructed from the samples.

Curiously, however, if it were possible to access other transformed samples of the signal, then it might be possible to gather enough information from both (or more) sets of samples and, therefore, reconstruct the signal. This motivated the function and derivative oversampling study discussed in Chapter 3. This chapter is mainly centered in sampling theory and, hence, the recovery of lost samples are studied under the assumption of oversampling. For the specific case of function and derivative oversampling, a stability study has also been included. These issues gave rise to [40, 41, 42] where the oversampling expansion for the function and derivative filter bank was established and the stability of the system with erasures was studied.

A very simple example of function and derivative reconstruction is the situation where one desires to establish the law of motion of, say, a car. But if there is not enough information about the position of the car and if it were possible to access sufficient information about the velocity of the car, then it would be possible to establish its law of motion. Thus, the function (position) and derivative (velocity) samples as a set allow for the reconstruction of the car's motion.

The function and derivative oversampling study is inherently structured around a two-channel filter bank, where one of the analysis filters returns samples of the signal and the other returns samples of its derivative. Here the two-channel structure arises again, as in the case of the two-channel DFT codes. The extension to multichannel sampling [7, 24] (sampling with two or more filter banks) from the two-channel case is somewhat

natural and roughly outlined in the transition from the classical (single channel) case to the two-channel one.

In the context of function and derivative oversampling, reconstruction from missing samples is studied. When the oversampling rate is large enough so that both channels alone are oversampled, then this reduces to the classical setup [16, 17] and the missing samples can always be recovered. However, when the oversampling rate is just above critical, both channels alone are undersampled and recovery of lost data becomes a more delicate matter. If samples are missing from only one of the channels (only function samples or only derivative samples), then the other channel compensates for the lost data and, therefore, the signal is always recovered. Curiously, however, when samples are lost from both channels simultaneously, the recovery of the lost samples may not always be possible, jeopardizing the reconstruction of the signal. This comes in clear contrast with the single channel case and the classical sampling theorem [16, 17, 31]. The system is shown to be very unstable for losses that affect both channels, even when recovery of the missing data is possible in principle. This is an important aspect to take into account, especially when the analysis filters are constructed by truncation.

It is interesting to notice how the introduction of a second channel in the continuous case of function and derivative oversampling, as well as in the discrete case of DFT codes, changes the stability of the erasure system quite dramatically. For the first case, the two-channel structure performs badly and even reconstruction is jeopardized when sample loss affects both channels. In contrast, for DFT codes the two-channel structure performs remarkably well even for bursty losses.

Following our works [40, 41], J. M. Kim and K. H. Kwon generalized the results for filter banks with two arbitrary channels [26]. Kim and Kwon studied the possibility of reconstructing a signal when samples are lost from only one channel or from both channels and present sufficient conditions that guarantee reconstruction. These conditions depend on the Lesbesgue measure of a certain set E and is denoted by $|E|$. This set consists of certain constraints which the transfer matrix must satisfy. The Lesbesgue measures of the positive side and negative side of the band, $|B_+|$ and $|B_-|$ respectively, are also important.

The notation $B + \pi$ is used to denote the set $B + \pi = \{b + \pi : b \in B\}$. The results presented in [26] allow a better understanding of the results obtained for the functional and derivative case [40, 41].

An application of the study of filter banks with undersampled channels is, for example, in multicoil MRI (parallel MRI techniques) in the iterative reconstruction of images from undersampled MRI data acquired by multiple receiver coil systems (which are actually the channels). The acquisition of undersampled data is important for speed, which is crucial in medical situations. Other applications can be related to motion and speed, energy and potential, momentum and force and so on.

1.1.3 Redundancy in DNA Sequences

A different domain but with an interesting application of the error-locating polynomial mentioned in Section 1.1.1 is in the context of DNA sequences discussed in Chapter 4. DNA sequences may be expressed as strings of the alphabet given by $\{A, C, G, T\}$. The positions of each symbol of the alphabet in a string can be identified by its respective indicator sequence, a binary sequence of zeros and ones, where 1 is assigned to each position of that symbol in the string. The idea of the indicator sequence arises from the necessity of representing each symbol numerically, so that periodicities and structures inherent to the sequence can be studied. However label invariance is essential, i.e., the symbol-to-number mapping should not introduce structures that do not exist in the symbolic sequence. Since the indicator sequences only distinguish between different symbols with no further assumption, they are a reasonable choice. It turns out that they arise naturally when searching for a meaningful spectrum definition for symbolic sinals [1].

The four indicator sequences (one sequence for each different symbol) are obviously redundant, since they all add up to 1. Furthermore, the redundancy present in the spectral components of each indicator sequence was found to be described by the error-locating polynomial, allowing for the prediction of subsequent symbols. More precisely, if there are m occurrences of a symbol in a sequence of length n, then the n spectral coefficients of the respective indicator sequence can be determined from any contiguous set of m occur-

rences via the linear recursion involving the coefficients of the polynomial as is described in Chapter 4. In other words, if a certain symbol appears m times in a string of length n, then any m contiguous spectral coefficients determine the remaining $n - m$ coefficients by the recursion. This issue gave rise to [2]. An overview of Fourier analysis applied to DNA sequences is given in [1].

1.1.4 Integrate-and-Fire Converter

Still in the context of reconstruction and specifically for the integrate-and-fire converter model presented in Chapter 5, a stable reconstruction procedure based on iterative POCS sequences is given for reconstructing both continuous [23] and discrete signals. Integrate-and-fire converters are motivated by the fact that some applications require low-cost and low-power devices at the encoder, trading off for more complex and high-cost decoding and reconstruction. This presents a new perspective of signal reconstruction, especially in the area of analog electronics. The idea for the case of continuous signals is to integrate the signal until its value reaches a certain threshold. Then at that instant an action is triggered and the integration is reset to zero. The discrete case is somewhat different, but the essential idea of summing until a threshold and firing at some instant is present. For both the continuous and discrete case, an alternating projections iterative method is presented which allows the recovery of the signal.

1.2 Contributions

The contributions of this thesis include: the study of error detection with random matrices [48] (Chapter 2); the establishment of the oversampling series expansion for the function and derivative filter bank, the study of the reconstruction of the original signal when a finite or infinite number of missing samples are lost and of the stability of the system (Chapter 3) which gave rise to [40, 41]; the relationship between the error-locating polynomial and the DNA indicator sequences (Chapter 4) which was reported in [2] and a survey into Fourier analysis on DNA sequences provided in [1]; and the presentation of an iterative method for stable reconstruction of discrete signals in the integrate-and-fire

converter model, following the line of thought for continuous signals [23] which is currently submitted for publication (Chapter 5).

Chapter 2

From DFT Codes to Random Codes

2.1 Introduction

Discrete Fourier transform (DFT) codes, a particular case of real number codes, are defined over the real or complex field and, thus, can be implemented using standard digital signal processors. They have been recognized as efficient for joint source and channel coding using signal processing techniques [29]. However DFT codes are not stable under bursty losses, since their numerical stability critically depends on the distribution of these erasures. In fact, contiguous erasures are very difficult to handle with DFT codes [22, 34, 36, 47].

It is common to distinguish erasures from errors. Erasures are errors that occur at known locations. These errors can be ignored and treated as lost samples at the respective position. Hence, the name erasures. Errors refer to those corrupted samples that occur but whose positions are not known and, therefore, cannot be immediately treated as lost samples.

To overcome the stability problems that DFT codes face with critical losses, the code is redesigned around a two-channel structure. Moreover, in one of the channels an interleaver or permutation is introduced. Each channel itself employs a DFT code. Therefore, the new code is a somewhat random version of the DFT code.

It is known that the two-channel code has a far better numerical stability than the respective DFT code [22, 47]. In fact, even in the ill-posed situation of bursty losses, the condition numbers of the decoding linear operators for the two-channel system can be smaller by several orders of magnitude than the condition numbers of the corresponding

operators for the DFT codes of the same rate. Clearly this performance must be due to the interleaver in the two-channel structure, which introduces some level of randomness. Nevertheless, the role that the interleaver plays in such an improvement is not completely clear from a mathematical point of view. What is clear is that randomness plays a key role in good stability. To corroborate this statement, [9] suggested codes based on random gaussian matrices and showed how these codes were very stable. However only the correction of erasures was addressed and not the detection of errors. This latter issue led to the development of [48].

2.2 DFT Codes

DFT codes can be implemented using standard arithmetic, in contrast with conventional error-correcting codes which are defined over finite fields (Galois fields). Thus they can be implemented with standard digital signal processors and, therefore, lead to efficient techniques for joint source-channel coding. Moreover, the severe restrictions concerning the size of the encoder input and output block lengths (K and N, respectively), known to finite field codes, no longer exist with real number codes.

In a DFT code, the original signal vector $a \in \mathbb{K}^K$ (vector with K samples) is zero padded and transformed (coded) to obtain an output vector $z \in \mathbb{K}^N$ (with N samples), where N is usually much greater than K ($\mathbb{K}$ denotes $\mathbb{R}$ or $\mathbb{C}$). Formally,

$$z = F_N \begin{pmatrix} a \\ 0 \end{pmatrix},$$

where F_N denotes the DFT transform matrix of order N,

$$(F_N)_{jk} = \frac{1}{\sqrt{N}}\ e^{-i2\pi jk/N}, \qquad j,k = 0,...,N-1,$$

and 0 denotes a vector of $N-K$ zeros. Schematically, this is shown in Figure 2.1.

If the following partition of F_N is considered

$$F_N = (\, G_{N\times K} \quad H_{N\times(N-K)}\,) \tag{2.2.1}$$

then

$$z = F_N \begin{pmatrix} a \\ 0 \end{pmatrix} = G_{N\times K} a.$$

The original signal a can then be obtained from z via F_N^H or equivalently by the pseudo-inverse of $G_{N\times K}$ denoted by $G_{N\times K}^{\dagger}$ and given by $(G_{N\times K}^T G_{N\times K})^{-1} G_{N\times K}^T$.

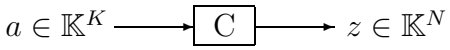

Figure 2.1: DFT coder. The vector a is zero padded to obtain an N-dimensional vector.

It is usually more convenient, in practice, to preserve the conjugate symmetry inherent to the DFT of real data ($\mathbb{K} = \mathbb{R}$) and, thus, take $K = 2M + 1$ (for some $M \in \mathbb{N}$). In this case the zeros are inserted in such a way that z remains real.

Sometimes samples from z can get corrupted and lost, jeopardizing the retrieval of a. However it may still be possible to recover these samples. In fact, the set of outputs of the code is a subspace of $\mathbb{K}^N$ of dimension K and is called the code subspace. Considering B as

$$B = F_N \begin{pmatrix} I & 0 \\ 0 & 0 \end{pmatrix} F_N^H = G_{N\times K} G_{N\times K}^H, \tag{2.2.2}$$

where I denotes the identity matrix of order K, it holds that $z = Bz$. The operator B can, thus, be understood as a projector onto the code subspace. It is precisely because z is confined to a proper subspace of $\mathbb{K}^N$ that error detection and correction becomes possible, since the observed vector z_0 (the vector z with corrupted samples) will not in general belong to the code subspace.

2.2.1 Correcting Erasures

Assuming that some samples of z have indeed been lost or corrupted by noise, consider J to be the set of the positions of the known samples and consider $\{B_i\}_{i=0}^{N-1}$ to be the columns of B. Note that since J is known, the lost samples are in fact erasures. If $|J| \geq K$, then

$\{B_i\}_{i\in J}$ is a frame for the code subspace. This means that there exist $\alpha, \beta > 0$ such that

$$\alpha\|z\|^2 \leq \sum_{i\in J} |\langle z, B_i\rangle|^2 = \|DBz\|^2 \leq \beta\|z\|^2$$

is satisfied, where D denotes the $N \times N$ diagonal matrix such that

$$D_{ii} = \begin{cases} 1, & i \in J \\ 0, & i \notin J. \end{cases} \tag{2.2.3}$$

It holds that $\alpha = \lambda_{\min}(BDB)$ and $\beta = \lambda_{\max}(BDB)$ are the tightest bounds, where $\lambda_{\min}(BDB)$ denotes the smallest nonzero eigenvalue of BDB and $\lambda_{\max}(BDB)$ denotes the largest eigenvalue of BDB. Then the observed signal is given by $z_0 = Dz$ and, hence, z can be recovered by the iteration

$$z_{n+1} = z_0 + (I - D)Bz_n \tag{2.2.4}$$

or, equivalently, by the equation

$$z = z_0 + (I - D)Bz.$$

Note that the recovery is only possible when $|J| \geq K$. In these conditions, however, if the losses are bursty (consecutive missing samples) the performance of the algorithm degrades or, equivalently, the condition number of BDB which is given by $\kappa = \beta/\alpha$ explodes, leading to an ill-posed situation and making the recovery of z practically impossible.

2.2.2 Locating Errors

In practice, the set J may not always be known. In other words, the positions of the corrupted samples as well as the number of these samples may not be known. In this situation, J must be determined. Because DFT codes are cyclic, they can be used to detect errors by means of the error-locating polynomial mentioned below.

Let $\overline{J} = \{i_0, ..., i_{n-1}\}$ be the positions of the unknown samples. Recall that $\overline{J}$ is unknown and, hence, must be determined. The number n, also unknown, is considered to be the

maximum number of errors that is possible to locate. Let $P(z)$ be the error-locating polynomial given by

$$P(z) = \sum_{k=0}^{n} h_k z^k, \tag{2.2.5}$$

where $h_n = 1$. Furthermore, $P(z)$ satisfies the restrictions

$$P(e^{-i2\pi i_p/N}) = 0, \qquad 0 \leq p < n.$$

Then if $\{h_k\}_{k=0}^{n}$ can be determined from the observed vector z_0, the positions $\{i_p\}_{p=0}^{n-1}$ follow from the n roots of $P(z)$. Considering $A = \{j_1, ..., j_n\}$ a set of distinct integers, it holds that

$$\begin{aligned}
&P(e^{-i2\pi i_p/N}) = 0 \\
&\sum_{k=0}^{n} h_k e^{-i2\pi i_p k/N} = 0 \\
&\sum_{k=0}^{n} h_k e^{-i2\pi i_p k/N} e^{i2\pi i_p j_q/N} = 0, \qquad 1 \leq q \leq n \\
&\sum_{k=0}^{n} h_k \sum_{p=0}^{n-1} z_0(i_p) e^{-i2\pi i_p (k-j_q)/N} = 0, \qquad 1 \leq q \leq n,
\end{aligned} \tag{2.2.6}$$

where $z_0(i_p)$ denotes the sample (component) of z_0 in the i_p position. Equation (2.2.6) is equivalent to

$$\sum_{k=0}^{n} h_k \widehat{z_0}(k - j_q) = 0, \qquad 1 \leq q \leq n,$$

where $\widehat{z_0} = F_N z_0$. Recall that $h_n = 1$ and, thus,

$$\sum_{k=0}^{n-1} h_k \widehat{z_0}(k - j_q) = -\widehat{z_0}(n - j_q), \qquad 1 \leq q \leq n,$$

which leads to a system of n equations to determine the n coefficients $\{h_k\}_{k=0}^{n-1}$. The positions $\{i_p\}_{p=0}^{n-1}$ can then be determined.

Once J has been obtained, the problem of locating errors becomes the problem of recovering erasures, the topic of Section 2.2.1.

2.3 Parallel Concatenated Codes

To overcome the poor conditioning of DFT codes in the presence of bursty losses, the new codes are rearranged around a two-channel structure. Two-channel codes, one channel in which the data are coded similarly to the DFT code, and another channel in which the data are interleaved before coding, lead to a more uniform performance with respect to error patterns and introduces randomness into the structure.

Interleaving is a common way of protecting against contiguous losses which lead to extremely ill-posed problems. Permuting the data maps contiguous losses to scattered losses, improving the conditioning of the reconstruction problem. However, a structure less sensitive to variations in the error pattern cannot be obtained simply by interleaving the coded data in a single channel system, because there are patterns that would be mapped by the interleaver into a contiguous fashion. Therefore, a two-channel code is used, where the pattern of losses in both channels will be sufficiently different (for a good interleaver) as to avoid contiguous losses in both channels.

Schematically, the two-channel code can be depicted as in Figure 2.2. Note that there are two outputs: $x \in \mathbb{K}^N$ and $y \in \mathbb{K}^N$.

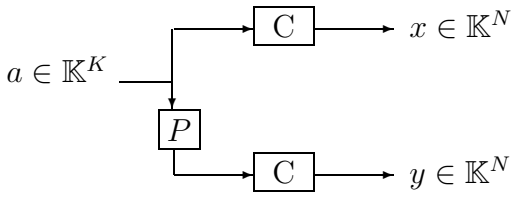

Figure 2.2: Two-channel coder. The interleaver is denoted by P.

The vector x is obtained from $a \in \mathbb{K}^K$ the same way as in the single channel case. But

the vector y is obtained from a by permuting its samples. More precisely,

$$\begin{aligned} x &= F_N \begin{pmatrix} a \\ 0 \end{pmatrix} = G_{N\times K} a \\ y &= F_N \begin{pmatrix} Pa \\ 0 \end{pmatrix} = G_{N\times K} Pa, \end{aligned}$$

where P denotes the permutation of order K. The result z is then obtained by the concatenation of x and y,

$$z = \begin{pmatrix} x \\ y \end{pmatrix}. \tag{2.3.1}$$

The corresponding DFT code output would be $z \in \mathbb{K}^{2N}$ such that

$$z = F_{2N} \begin{pmatrix} a \\ 0 \end{pmatrix} = G_{2N\times K} a,$$

where F_{2N} denotes the DFT matrix of order $2N$. The original vector a can then be retrieved via F_{2N}^H or, equivalently, $G_{2N\times K}^\dagger$.

Since there are two channels, losses can occur both in x and y. But the vectors can be recovered if the number of known samples in both channels is equal or greater than K. Considering B as in (2.2.2), it holds that $x = Bx$ and $y = By$. In turn, taking T to be

$$T = F_N \begin{pmatrix} P & 0 \\ 0 & 0 \end{pmatrix} F_N^H = G_{N\times K} P G_{N\times K}^H, \tag{2.3.2}$$

it holds that $y = Tx$, $TT^H = B$ and $TB = BT = T$. Note that both B and T are projectors and, thus, will allow for the localization and correction of errors.

2.3.1 Correcting Erasures

Let J_1 denote the set of the positions of the known samples in the first channel and J_2 denote the set of the positions of the samples known in the channel with the interleaver. Moreover, let D_i be the $N \times N$ diagonal matrix such that

$$(D_i)_{jj} = \begin{cases} 1, & j \in J_i \\ 0, & j \notin J_i \end{cases} \qquad i = 1, 2.$$

Then the missing samples can be recovered if $|J_1 \cup J_2| \geq K$. In this situation, we consider the frame $\{B_i\}_{i\in J_1} \cup \{T_i\}_{i\in J_2}$. Note that in this case

$$\alpha\|x\|^2 \leq \sum_{i\in J_1} |\langle x, B_i\rangle|^2 + \sum_{i\in J_2} |\langle x, T_i\rangle|^2 = \|D_1 Bx\|^2 + \|D_2 Tx\|^2 \leq \beta\|x\|^2$$

and, thus, the frame bounds α and β follow from the eigenvalues of $BD_1B + T^H D_2 T$.

The observed signals x_0 and y_0 (signals with missing samples) are given by $x_0 = D_1 x$ and $y_0 = D_2 y$. Recalling that $y = Tx$, the vectors x and y can be recovered by the alternating projection iteration given by

$$\begin{cases} x_{n+1} = x_0 + (I - D_1)Bx_n \\ y_{n+1} = Tx_{n+1} \\ y_{n+2} = y_0 + (I - D_2)By_{n+1} \\ x_{n+2} = T^H y_{n+2} \end{cases} \tag{2.3.3}$$

or, equivalently, by the system

$$\begin{cases} y = Tx_0 + T(I - D_1)Bx \\ x = T^H y_0 + T^H(I - D_2)By. \end{cases}$$

In practice, this algorithm performs remarkably well, even for contiguous losses, a situation which leads to ill-conditioning in the single channel case.

2.3.2 Locating Errors

As mentioned in Section 2.2.2, the set of the positions of the corrupted or lost samples may not be known. It is, therefore, necessary to locate the errors in the observed vectors x_0 and y_0.

If J is taken to be $J = J_1 \cup J_2$ and z is given by (2.3.1), then the procedure described in section 2.2.2 is straightforward and, hence, the positions of J_1 and J_2 can be determined. The problem is then reduced to the correction of erasures, discussed in Section 2.3.1.

2.4 Random Codes

The randomness introduced by the permutation seems to be essential for good performance. This motivated the study of random codes based on the gaussian distribution,

taking the random factor to extreme since the respective matrices do not have any specific structure. In fact, these random codes perform quite well, independently of the erasure pattern [9]. Actually, they outperform the two-channel codes impressively. Real and complex random matrices have been proposed, although only real matrices are treated here (for the sake of simplicity).

Let F_N be an $N \times N$ random gaussian matrix (the entries are based on a gaussian distribution) and consider the partition given by (2.2.1) (here F_N denotes the random matrix and not the Fourier matrix of the above sections; the notation is maintained for the sake of comparison). Then the coded vector z is obtained from $a \in \mathbb{R}^K$ as

$$z = F_N \begin{pmatrix} a \\ 0 \end{pmatrix} = G_{N\times K} a. \tag{2.4.1}$$

Schematically, this can also be depicted by Figure 2.1.

2.4.1 Correcting Erasures

Let J be the set of the positions of the known samples of z, assuming that there is sample loss or corruption. Then the known vector z_0 can be expressed as

$$z_0 = Dz = DG_{N\times K} a$$

where D is given by (2.2.3). If $|J| \geq K$, then a can be recovered by solving the subsystem of (2.4.1) given by

$$a = (DG_{N\times K})^{\dagger} z_0$$

and hence z can also be recovered. Taking B to be the matrix (cf. (2.2.2))

$$B = F_N \begin{pmatrix} I & 0 \\ 0 & 0 \end{pmatrix} F_N^{-1},$$

z can be recovered iteratively as

$$z_{n+1} = z_0 + (I - D)Bz_n$$

or by the system

$$z = z_0 + (I - D)Bz.$$

These codes have been shown to be very stable with high probability. In fact, the condition number for F_N ($N > 1$ and $t > 1$) satisfies [9]

$$\frac{0.13N}{t} < P(\kappa(F_N) > t) < \frac{5.60N}{t}$$

and $E(\log \kappa(F_N)) = \log(N) + c + \epsilon_n$ with $c \approx 1.537$ and $\lim_n \epsilon_n = 0$. Moreover, the condition number for $G_{N\times K}$ ($N \geq K \geq 2$) satisfies [10]

$$E(\log \kappa(G_{N\times K})) < \log \frac{N}{N - K + 1} + 2.258.$$

2.4.2 Locating Errors

Since F_N has no particular structure, if J is not known then at first sight the recovery of z may seem impossible. However by means of the syndrome and under certain circumstances, it is possible and even feasible to recover z. The matrix F_N can be considered to be orthogonal without loss of generality (else the matrix can be orthogonalized by a QR factorization using Gram-Schmidt orthogonalization). In this case, it is always true that $H^T_{N\times(N-K)}G_{N\times K} = 0$, where $H_{N\times(N-K)}$ is defined in (2.2.1).

Let z_0 be the observed signal, $z_0 = z + e$ where e is a sparse error vector with $L = |J|$ samples different from zero and J is unknown. Then the syndrome is given by

$$s = H^T z_0 = H^T(z + e) = H^T(G_{N\times K}a + e) = H^T e$$

and only depends on the error vector (H^T denotes $H^T_{N\times(N-K)}$ for simplicity). The error vector e can then be recovered by solving the underdetermined system $H^T e = s$. Since the system has many solutions, the sparsest solution is intended for practical purposes. This is, however, a combinatorial problem which can be formulated as

$$(\mathrm{P}_0) \quad \min \|e\|_0 \quad \text{subject to} \quad H^T e = s,$$

where $\|e\|_0 = \#\{i \in \{1,..,N\} : e_i \neq 0\}$ is the ℓ_0-norm (pseudo-norm). This problem has a unique solution if the vector e is sufficiently sparse. More precisely, if $\|e\|_0 = L$, then e is the unique solution of (P_0) if and only if [28]

$$L < \frac{K(H^T)+1}{2},$$

where $K(H^T)$ is the ambiguity index of H^T and is defined as the largest number such that *any* set of $K(H^T)$ columns of H^T is linearly independent. This bound is well known in coding theory as the Singleton bound [5]. Indeed, note that $K(H^T) \leq N - K$ and so $L < (N-K+1)/2$ or equivalently $L \leq (N-K)/2$. To construct a code capable of correcting t errors, two new samples must be added to the message vector a, $N - K = 2t$.

The system $H^T e = s$ can still be expressed as

$$\begin{pmatrix} h_1 & \cdots & h_N \end{pmatrix} \begin{pmatrix} e_1 \\ \vdots \\ e_N \end{pmatrix} = s$$

where $\{h_i\}_{i=1}^N$ represent the columns of H^T. It is easy to see that the syndrome can be written as a linear combination of those columns,

$$s = \sum_{i=1}^{N} h_i e_i.$$

The question that arises is: how can the combinatorial nature of (P_0) be circumvented to retrieve e? Donoho and Elad [13, 15] showed that in certain conditions, (P_0) can be solved by the linear programming problem given by

$$(\mathrm{P}_1) \quad \min \|e\|_1 \quad \text{subject to} \quad H^T e = s,$$

where $\|e\|_1 = \sum_i |e_i|$ is the ℓ_1-norm. This problem can be solved efficiently even for large N by using interior-point algorithms [6, 11, 53].

Assume (without loss of generality) that H^T is normalized, i.e., $\|h_i\|_2 = 1$, $i = 1, ..., N$. If $\|e\|_0 = L < ebp$, where

$$ebp = \frac{1 + 1/M(H^T)}{2}$$

and $M(H^T) = \max_{i \neq j} |h_i^T h_j|$, then ($P_0$) is equivalent to ($P_1$), i.e., the solution of (P_1) is the solution of (P_0). The mutual incoherence of H^T, $M(H^T)$, measures the distribution of the frame vectors of H^T. Note that $M(H^T) \in [0, 1]$ and that $M(H^T) \approx 1$ if the vectors are almost collinear. In turn, the equivalence break point, *ebp*, is the maximum number of errors that the code is guaranteed to correct.

It is well known that if $K(H^T) = N - K$ (not without significance, since we are dealing with random matrices) then the following holds for the mutual incoherence [52],

$$M(H^T) \geq \sqrt{\frac{K}{(N-K)(N-1)}} = M_{\text{opt}}.$$

$M(H^T)$ measures how spread-out the columns of H^T are and, in this case, $M(H^T) = 0$ if H^T has orthogonal columns. If $M(H^T) = M_{\text{opt}}$ then it is expected that the code generated by such a matrix achieves good results. Such matrices are known as Grassmannian frames [12, 44] and have the vectors $\{h_i\}$ distributed in an optimal way (in the sense of the angles between the vectors). The equivalence break point in this case is optimized,

$$ebp_{\text{opt}} = \frac{1 + 1/M_{\text{opt}}}{2}$$

and the code is, thus, expected to perform much better than a random code chosen arbitrarily. This however is not true since in some cases the random frames perform better, as confirmed by Figure 2.3. A syndrome for a positive valued error pattern was generated and the sparse error solution was obtained by solving (P_1) via an interior-point algorithm. For each number of errors, 10^5 error patterns were tested and the number of successfully retrieved error vectors was counted. In this case, the random code outperformed the Grassmannian code, contrary to what was expected. The number of errors successfully corrected is well above the *ebp* threshold, suggesting that this bound is a very conservative one.

The mutual incoherence reflects the worst case and more insight is provided by the histogram of the off diagonal elements of the Gram matrix, HH^T, which represent the dot products $|h_i^T h_j|$. In Figure 2.4, it can be noted that the frame angles for the random

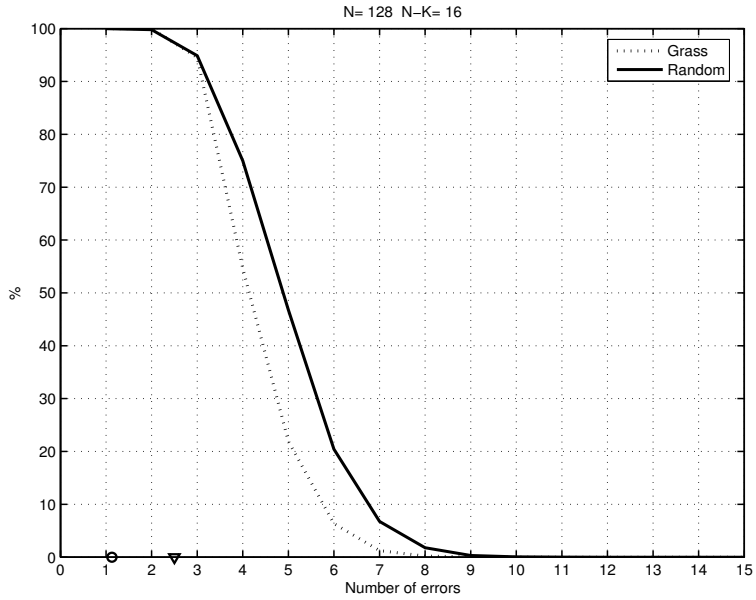

Figure 2.3: Percentage of corrected error patterns for several numbers of errors. $\circ$ and $\triangledown$ represent the *ebp* for the random code and the Grassmannian code, respectively.

matrix assume values between 0 and 0.75, whereas the maximum dot product for the Grassmannian matrix is 0.25. It is, thus, obvious that the angles between the frame vectors do not hold all the information about the frame subspace. Actually the angles between the subspaces formed by $\{h_i\}$ must also play a role in explaining the performance of the codes, although this issue is also of combinatorial nature.

One of the problems in solving (P_1) as a linear programming problem, is that all the errors should be positive. To circumvent this limitation, let $e_i^+ = \max\{e_i, 0\}$ and $e_i^- = \max\{-e_i, 0\}$ with $i = 1, ..., N$. Then $e = e^+ - e^-$ and can be recovered by a variant of (P_1) given by

$$(P_1') \quad \min \|\tilde{e}\|_1 \quad \text{subject to} \quad (\, H^T \quad -H^T \,)\, \tilde{e} = s \quad \text{and} \quad \tilde{e} \geq 0$$

with $\tilde{e} = (\, e^+ \quad e^- \,)^T$.

2.5 Stability

It is a fact that the numerical stability of DFT codes depends critically on the distribution and magnitude of the errors. In particular, for bursty losses, these codes are extremely

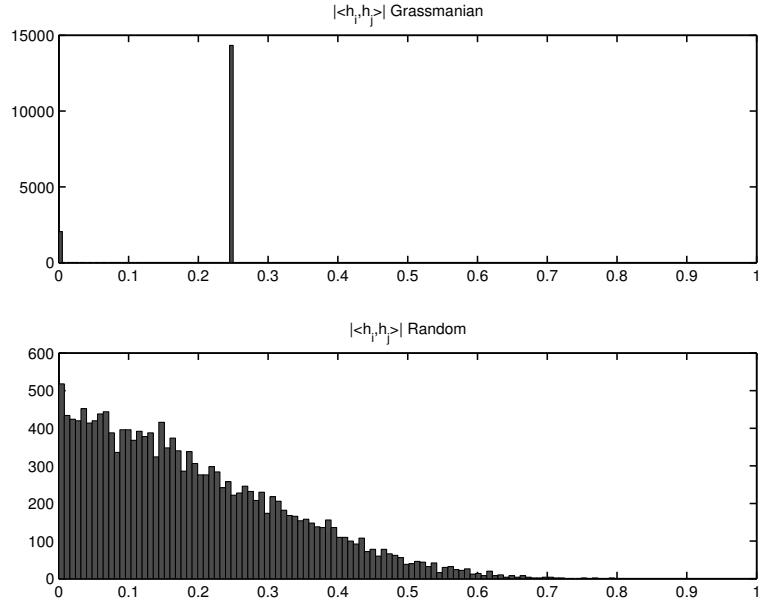

Figure 2.4: Histograms of all angles between the frame vectors. The top plot is for the Grassmannian matrix and the botton one is for the random matrix.

unstable. Formally, since the condition number of BDB given by $\kappa = \beta/\alpha$ measures the stability of the system, if J is contiguous then $\alpha \approx 0$, leading to an ill-conditioned situation which is traduced by a very large κ. This means that the algorithm given by (2.2.4) degrades dramatically for bursty erasure patterns.

In contrast, when the codes are arranged in a two-channel structure with an interleaver, the algorithm given by (2.3.3) performs remarkably well, even for contiguous losses. In fact, the condition number for the two-channel case can be smaller by several orders of magnitude when compared to the single channel case. However, the random code seems to be far better conditioned. Figure 2.5 shows the condition number of a DFT code, its parallel concatenated counterpart and a random code, for $N = 256$ ($N = 128$ in each channel for the two-channel code) and $K = 21$, as the number of bursty losses increases. The condition number for the random code never exceeds 10, whereas for the DFT code it explodes quickly. The two-channel code is far more stable than the DFT code (by up to six orders of magnitude), although the random code leads in stability.

Mathematically, the much better performance of the two-channel code with respect to the DFT code, is not fully understood. However, in practice, it is possible to verify that

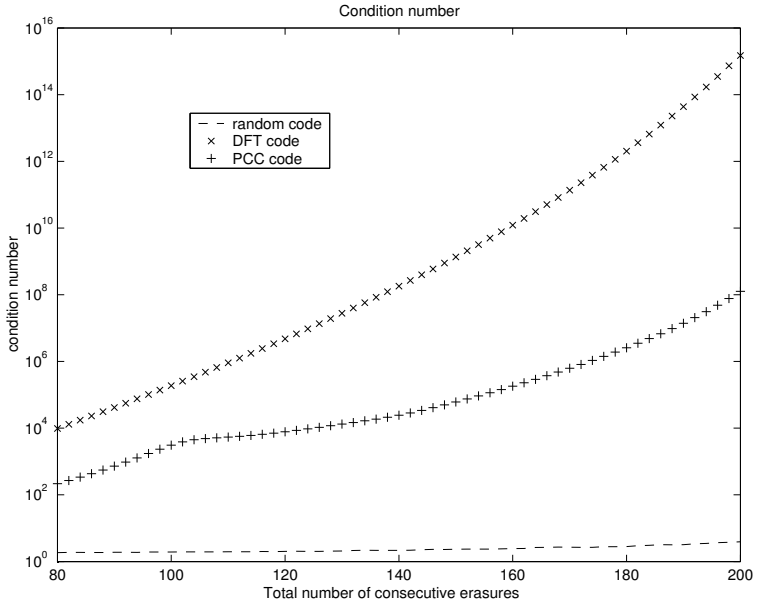

Figure 2.5: Log plot of the condition number versus the total number of consecutive missing samples $|J|$ for the DFT code ($N = 256$), the two-channel counterpart ($N = 128$ and $|J|/2$ missing samples per channel) and a random code ($N = 256$) with K=21.

for the DFT code the smallest nonzero eigenvalue is difficult to detect from the noise floor (theoretical zero eigenvalues), whereas this is not true for the two-channel case nor for the random case. Hence, the permutation and randomness intervene in keeping the smallest nonzero eigenvalue well above the noise floor, as can be confirmed by Figure 2.6. It is a fact that the frame $\{B_i\}_{i\in J_1} \cup \{T_i\}_{i\in J_2}$ is generally far more robust to erasures than the single channel frame $\{B_i\}_{i\in J}$, confirming the importance of the presence of the interleaver and, thus, of the scattering of contiguous patterns. Thus, randomness seems to be essential for good stability.

2.6 Conclusion

In the context of DFT codes, it was described how the problem of locating errors can be reduced to the problem of correcting erasures, once the error positions were determined by means of the roots of the error-locating polynomial given by (2.2.5). In turn, when erasures occur or, in other words, when samples are lost and their positions are known, these samples can be recovered via the matrices B and D given by (2.2.2) and (2.2.3) respectively, as

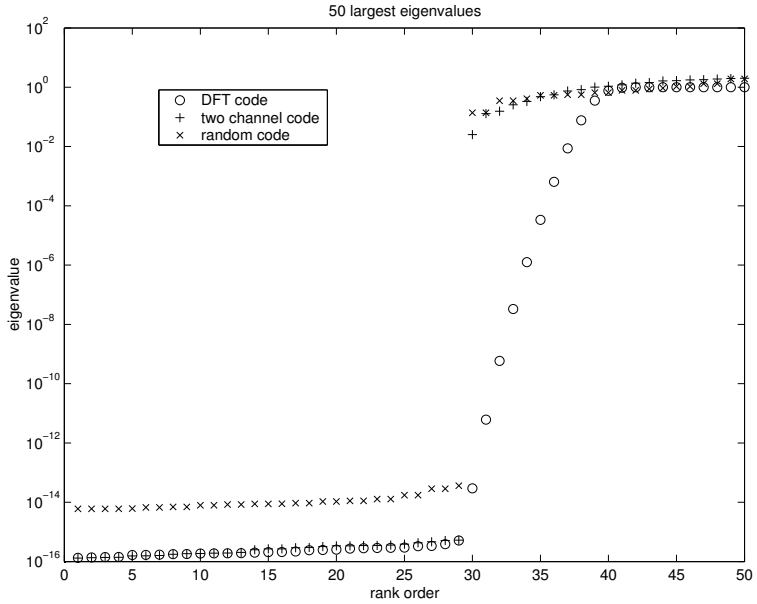

Figure 2.6: Log plot of the 50 largest eigenvalues for the DFT code ($N = 128$ and $|J| = 68$), for the two-channel code ($N = 64$ and $|J| = 34$ per channel) and for the random code ($N = 128$ and $|J| = 68$) with K=21.

long as the number of known samples is equal to or greater than K (the dimension of the original vector a). However, the stability of the recovery of missing samples depends critically on the distribution of the erasures and, in particular, is very poor for contiguous loss patterns.

This fact motivated the two-channel DFT code structure with an interleaver, which provides randomness to the code. In this case, the error-locating problem is reduced to the erasure-correcting problem the same way as described for the DFT code. However, the correction of erasures now involves not only matrix B but also matrix T given by (2.3.2) (which has the interleaver P), as well as the erasure position matrices D_1 and D_2. Surprisingly, the stability of the reconstruction by the two-channel system is remarkably good, even for the contiguous erasure pattern case.

It is clear that the interleaver is important for improving stability and is responsible for scattering contiguous patterns. Very structured interleavers (such as transpositions) lead to poor scattering and, thus, do not improve stability significantly. Nevertheless, a mathematical demonstration of how the interleaver interferes in the condition number of the system has not yet been provided.

Taking randomness to extreme, random codes based on the gaussian distribution were presented. These codes outperform the two-channel codes with impressive stability, independently of the erasure pattern. Because the matrix involved presents no specific structure, error detection may seem impossible. However, the problem can be formulated as the combinatorial problem (P_0) and can be solved as the linear programming problem (P_1) or (P_1'), provided that the conditions of sparsity are met. The performance of these codes depends on the angles of the subspaces formed by the frame vectors $\{h_i\}$.

Chapter 3

Two-Channel Oversampling

3.1 Introduction

Two-channel sampling, a particular case of multichannel sampling [7, 24], is motivated by the fact that sometimes one may have samples relative to a certain (bandlimited) signal f, but not sufficiently dense (sampled at a rate lower than the critical rate). However, if it were possible to have access to other transformed samples of f, then it could be possible to reconstruct the signal. For example, consider a car that follows a certain trajectory. One would have a list of certain locations the car passed, but it may not be sufficient to establish the law of motion of the car. However, if at each location known one could also measure the velocity (with radars), then the law of motion could be established (if the samples of position together with those of velocity were sufficiently dense). This example is a particular occurrence of function and derivative sampling. Other examples include situations involving momentum and force, current and charge, energy and potential and so on.

An interesting application of the study of filter banks with undersampled channels may be, for example, multicoil MRI (parallel MRI techniques). Here images are reconstructed from undersampled MRI data acquired by multiple receiver coil systems (which are actually the channels). The reason for undersampled data is that of speed, which is crucial in medical situations.

Thus sometimes a second channel is sufficient to retrieve the desired signal. More channels can be added (a topic of multichannel sampling). The two-channel structure

has also revealed to be more robust to erasures in certain conditions, such as in the two-channel DFT codes [20, 21, 35, 39, 45] (a discrete case of two-channel sampling) discussed in Chapter 2. In this context, the two-channel structure presents much better stability than the respective DFT code [22, 38]. Note however that the DFT codes deals with block codes of a finite number of samples whereas filter bank oversampling deals with samples of a continuous time function.

The two-channel filter bank (Fig. 3.1) consists of two analysis filters, h_1 and h_2, which convolve with a bandlimited signal f ($\text{supp}(\hat{f}) \in [-\omega_a, \omega_a]$ for some $\omega_a > 0$, where $\hat{f}$ denotes the Fourier transform of f and $\text{supp}(\hat{f}) = \{\omega : \hat{f}(\omega) \neq 0\}$). The result is then sampled. The synthesis filters, g_1 and g_2, are used to reconstruct f from the two sets of samples. If the filter bank is a critical one (the analysis filters are sampled at a critical rate), the loss or corruption of any sample will be severe, since the signal cannot be reconstructed. The importance of oversampled filter banks, in this case, is addressed in the next section.

The study of oversampled two-channel filter banks focusing, in particular, the function and derivative case gave rise to [40, 41]. The recovery of missing samples is analyzed and the stability of the recovery is studied. Generalizations of these results were presented by other authors in [26].

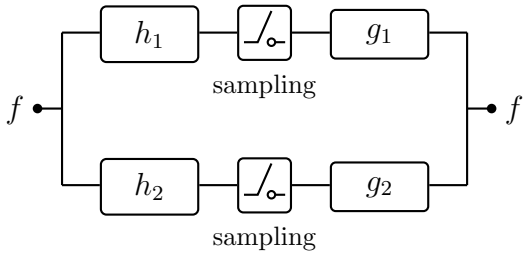

Figure 3.1: Two-channel sampling as a filter bank which consists of two analysis filters, h_1 and h_2, and two synthesis filters, g_1 and g_2.

3.2 The Importance of Oversampling

In practice, for example in real time multimedia transmission over IP networks, data loss can occur. To avoid retransmission of the signal and further delays, one can try to reconstruct the missing data from the received information. This can be done using

conventional error control coding or using techniques that are roughly equivalent to joint source-channel DFT codes. However, recovery of lost samples requires redundancy and, therefore, oversampled series expansions may also be used to recover the lost samples and obtain the original signal. These expansions are particularly advantageous when the signals have already been oversampled, thus avoiding the introduction of further redundancy via conventional channel coding (for example, zero padding).

Oversampling is present when the system is sampled at a rate higher than the critical or Nyquist rate ($2\omega_a$ Hz). If the system is sampled at the critical rate, then the loss of even one sample will yield reconstruction of f impossible. However, if the system is oversampled, then reconstruction of f may be possible.

In the classical sampling theorem (single channel case), when the system is oversampled exact recovery remains possible when any finite number of samples is lost [16, 17, 31], a fact that remains true even for the Kramer sampling series [16].

In the two-channel case, assuming both channels have equal sampling rate (for simplicity), the system is critically sampled when each channel is sampled at the rate of ω_a Hz (the overall sampling rate adds up to $2\omega_a$ Hz). Thus, when each channel is sampled at a rate higher than ω_a Hz, the two-channel filter-bank is oversampled.

Let ω_s be the sampling frequency in each channel (the overall sampling rate adds up to $2\omega_s$). Define r to be the oversampling parameter which is given by $\omega_a = r\omega_s$. Since there is oversampling, r must satisfy $0 < r < 1$. When $r < 1/2$, each channel alone is an oversampled system and, hence, each channel can recover the missing samples independently. The study of this case is then reduced to the study of the single channel case [16, 17]. In turn when $r = 1/2$, each of the channels are critically sampled and, hence, if no data loss occurs, each channel alone is capable of reconstructing the signal. However, if data loss does occur, both channels are required for reconstruction. If $1/2 < r < 1$, each channel is undersampled and, therefore, reconstruction of f requires samples from both channels. Thus, for $1/2 \leq r < 1$, recovery of missing samples may be possible only when samples from both channels are considered. This situation has revealed to be quite interesting and with results somewhat unexpected, since recovery is not always possible

when samples are missing from both channels simultaneously.

3.3 The General Case

In the general two-channel filter bank, one channel returns samples of $\{a(k)\}$ and the other returns samples of $\{b(k)\}$, where a and b are transforms of the signal f.

3.3.1 The Oversampled Expansion

The general sampling formula for two-channel sampling can be adapted to the oversampling case by projecting (filtering) onto the subspace of signals bandlimited to ω_a Hz. Assuming without loss of generality that $\omega_s = 1$ Hz and, thus, $\omega_a = r$, the reconstruction formula becomes

$$f(t) = \sum_{k=-\infty}^{\infty} a(k)s_1(t-k) + b(k)s_2(t-k), \tag{3.3.1}$$

where $a(k)$ and $b(k)$ are the sampled outputs of the analysis filters and s_1 and s_2 are the projections of their impulse responses on the subspace of signals bandlimited to r Hz, where $1/2 < r < 1$.

3.3.2 Reconstruction with Missing Samples

Consider $i_1, ..., i_n$ to be the positions of the missing samples in $\{a(k)\}_k$ and/or $\{b(k)\}_k$ (note that only erasures are studied, i.e., it is assumed that the error positions are known). Then, (3.3.1) can be presented in terms of the unknown samples,

$$f(i_m) \;=\; \sum_{k=1}^{n} a(i_k)s_1(i_m - i_k) + b(i_m)s_2(i_m - i_k) + h(i_m) \tag{3.3.2}$$

where

$$h(i_m) = \sum_{k \neq i_1,...,i_n} a(k)s_1(i_m - k) + b(k)s_2(i_m - k),$$

for $m = 1, .., n$. In matrix form, (3.3.2) can be expressed as

$$f = S_1 a + S_2 b + h,$$

where

$$(S_1)_{mk} = s_1(i_m - i_k) \qquad (S_2)_{mk} = s_2(i_m - i_k)$$

$$a = (\, a(i_1) \quad \cdots \quad a(i_n)\,)^T \qquad b = (\, b(i_1) \quad \cdots \quad b(i_n)\,)^T$$

$$h = (\, h(i_1) \quad \cdots \quad h(i_n)\,)^T .$$

If recovery of the missing samples is successful, then reconstruction of the signal f is possible. Such recovery is dependent on invertibility conditions associated to s_1 and s_2.

3.4 The Function and Derivative Case

The function and derivative case is a particular case of two-channel sampling, where one of the analysis filters returns samples of f and the other returns samples of f' (Figure 3.2). The study of such a case is motivated by the fact that, for example, one could have information about the position of a car from time to time, but not sufficiently to reconstruct the motion law. However, if information about the velocity was also available, then this information could be sufficient to fill in the gaps and recover the law of motion concerning the car. Many physical problems fit into the function and derivative framework (position vs velocity, charge vs current, momentum vs force and so on).

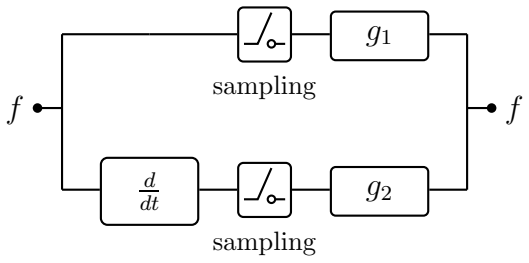

Figure 3.2: Function and derivative sampling as a filter bank.

3.4.1 The Oversampled Expansion

From the general two-channel case, the reconstruction of a finite-energy function f bandlimited to ω_a Hz from samples of itself and its derivative is possible when each of these are sampled at half the Nyquist rate, that is, ω_a Hz, and the reconstruction formula is given by [24]

$$\begin{aligned} f(t) &= \sum_{k=-\infty}^{\infty} \left\{ f\left(kT_a\right) \operatorname{sinc}^2\left[\omega_a\left(t-kT_a\right)\right] + \right. \\ &\qquad \left. f'\left(kT_a\right)\left(t-kT_a\right) \operatorname{sinc}^2\left[\omega_a\left(t-kT_a\right)\right] \right\}, \end{aligned} \tag{3.4.1}$$

where $T_a = 1/\omega_a$ and, as usual, $\operatorname{sinc}(x) = \sin(\pi x)/(\pi x)$. The oversampled version can, thus, be obtained by lowpass filtering the signal given in (3.4.1),

$$\begin{aligned} f(t) = \sum_{k=-\infty}^{\infty} & f\left(\frac{k}{\omega_s}\right) \left\{ 2r(1-r)\operatorname{sinc}\left[2r\omega_s\left(t-\frac{k}{\omega_s}\right)\right] + r^2\operatorname{sinc}^2\left[r\omega_s\left(t-\frac{k}{\omega_s}\right)\right] \right\} + \\ & f'\left(\frac{k}{\omega_s}\right) r^2 \left(t-\frac{k}{\omega_s}\right) \operatorname{sinc}^2\left[r\omega_s\left(t-\frac{k}{\omega_s}\right)\right], \end{aligned}$$

where ω_s is the sampling frequency. Assuming, as above, that $\omega_s = 1$ and, thus, $\omega_a = r$, this reduces to

$$f(t) = \sum_{k=-\infty}^{\infty} f(k)s_1(t-k) + f'(k)s_2(t-k), \tag{3.4.2}$$

where

$$s_1(t) = 2r(1-r)\operatorname{sinc}(2rt) + r^2\operatorname{sinc}^2(rt)$$

and

$$s_2(t) = r^2 t\operatorname{sinc}^2(rt)$$

(details are presented in Appendix A). Note that, as expected, (3.4.2) has the form of (3.3.1).

3.4.2 Reconstruction with Missing Samples

In the particular case of function and derivative sampling, $i_1, ..., i_n$ are the positions of the missing samples in $\{f(k)\}_k$ and/or $\{f'(k)\}_k$. Then (3.3.2) becomes

$$f(i_m) = \sum_{k=1}^{n} f(i_k)s_1(i_m - i_k) + f'(i_m)s_2(i_m - i_k) + h(i_m)$$

where

$$h(i_m) = \sum_{k \neq i_1,...,i_n} f(k)s_1(i_m - k) + f'(k)s_2(i_m - k),$$

for $m = 1, .., n$. It follows that

$$F = S_1F + S_2F' + h, \tag{3.4.3}$$

where $F = (\, f(i_1) \quad \cdots \quad f(i_n)\,)^T$ and $F' = (\, f'(i_1) \quad \cdots \quad f'(i_n)\,)^T$. The possibility of reconstruction depends on s_1 and s_2. These functions are represented in Figure 3.3.

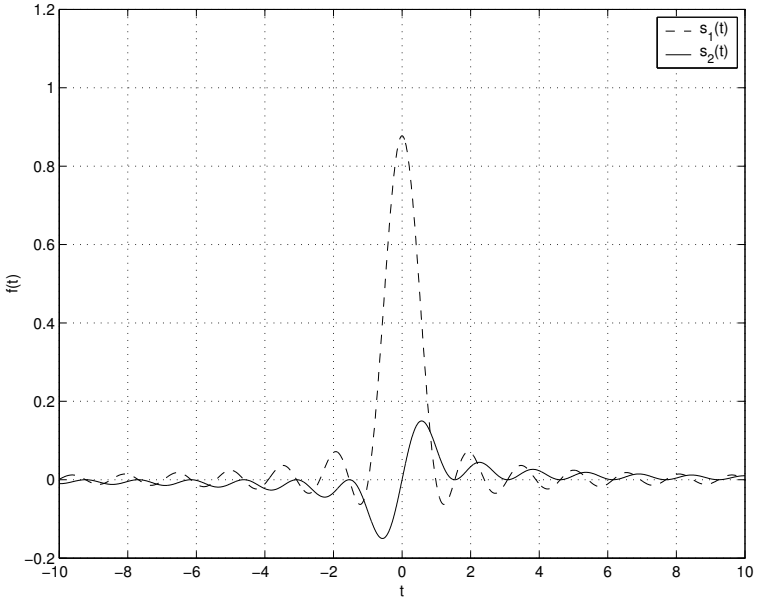

Figure 3.3: Plot of the functions s_1 and s_2 with $r = 0.65$.

3.4.2.1 Missing Function Samples

When the samples $\{f(i_k)\}_{k=1}^n$ are missing, but $\{f'(i_k)\}_{k=1}^n$ are known, then f can be obtained from (3.4.3) as

$$(I - S_1)F = S_2F' + h \tag{3.4.4}$$

as long as $I - S_1$ is invertible (S_1 and S_2 are $n \times n$ matrices). If $I - S_1$ is indeed invertible, then 1 cannot be an eigenvalue of S_1. This yields that the quadratic form of S_1 satisfies the condition $x^H S_1 x \neq \|x\|^2$, for $x \neq 0$. To see if this is true, for $x \neq 0$, one obtains that

$$\begin{aligned}
x^H S_1 x &= \sum_m \sum_k x_m^* x_k s_1(i_m - i_k) \\
&= \sum_m \sum_k x_m^* x_k \int_{-r}^{r} \hat{s}_1(\omega) e^{i2\pi\omega(i_m - i_k)} d\omega \\
&= \int_{-r}^{r} \hat{s}_1(\omega) \sum_m \sum_k x_m^* x_k e^{i2\pi\omega(i_m - i_k)} d\omega \\
&= \int_{-r}^{r} \hat{s}_1(\omega) \underbrace{\left| \sum_k x_k e^{i2\pi\omega i_k} \right|^2}_{M(\omega)} d\omega.
\end{aligned}$$

Since the function M is a periodic function with period of 1 Hz it follows that

$$\begin{aligned}
x^H S_1 x &= \int_{-r}^{-1/2} \hat{s}_1(\omega) M(\omega) d\omega + \int_{-1/2}^{1/2} \hat{s}_1(\omega) M(\omega) d\omega + \int_{1/2}^{r} \hat{s}_1(\omega) M(\omega) d\omega \\
&= \int_{1-r}^{1/2} \hat{s}_1(\omega - 1) M(\omega - 1) d\omega + \int_{-1/2}^{1/2} \hat{s}_1(\omega) M(\omega) d\omega + \\
&\quad \int_{-1/2}^{r-1} \hat{s}_1(\omega + 1) M(\omega + 1) d\omega \\
&= \int_{-1/2}^{1/2} \left[\hat{s}_1(\omega - 1)\chi_{[1-r,1/2]} + \hat{s}_1(\omega) + \hat{s}_1(\omega + 1)\chi_{[-1/2,r-1]} \right] M(\omega) d\omega,
\end{aligned}$$

where χ_A denotes the characteristic function of a set A,

$$\chi_A(x) = \begin{cases} 1, & x \in A \\ 0, & x \notin A. \end{cases}$$

Due to the fact that $1/2 < r < 1$, there are at most two overlaps. In this manner, $\hat{s}_1(\omega - 1)$ never overlaps with $\hat{s}_1(\omega + 1)$. The Fourier transform of s_1 is given by

$$\hat{s}_1(\omega) = 1 - |\omega|, \quad \omega \in [-r, r].$$

Hence, when the overlapping does occur either

$$\hat{s}_1(\omega) + \hat{s}_1(\omega - 1) = 1$$

is satisfied, or

$$\hat{s}_1(\omega) + \hat{s}_1(\omega + 1) = 1,$$

as can be confirmed by Figure 3.4. Moreover, there is a neighborhood around zero where overlapping is absent. Because of this,

$$x^H S_1 x < \int_{-1/2}^{1/2} M(\omega) d\omega = \|x\|^2.$$

Consequently $I - S_1$ is invertible and, therefore, recovery of the missing samples of $\{f(k)\}_k$ is possible.

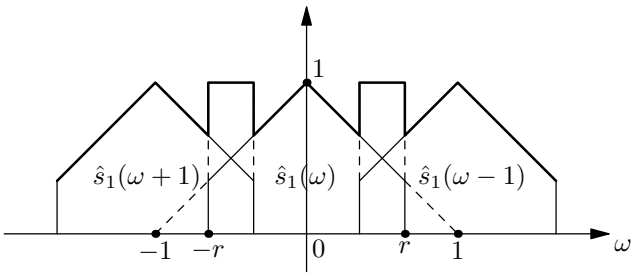

Figure 3.4: Spectral components of s_1. The thick line corresponds to the sum of the components.

3.4.2.2 Missing Derivative Samples

In turn, when the samples $\{f(i_k)\}_{k=1}^n$ are known and the missing ones are $\{f'(i_k)\}_{k=1}^n$, then (3.4.3) becomes

$$S_2F' = (I - S_1)F - h.$$

However S_2 is antisymmetric. For odd order, it can be verified that S_2 is singular. Then, this equation is not satisfactory for the recovery of $\{f'(i_k)\}_{k=1}^n$. But deriving (3.4.3) yields

$$F' = S_1'F + S_2'F' + h'$$

(S_1' and S_2' are $n \times n$ matrices). In this case, reconstruction depends on the derivatives of s_1 and of s_2, which are represented in Figure 3.5 (note the duality between s_1 and s_2' and between s_2 and s_1').

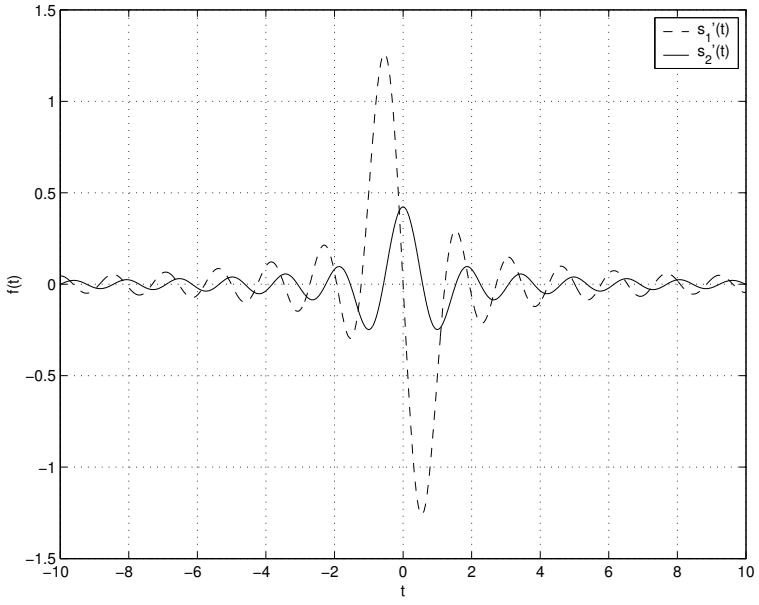

Figure 3.5: Plot of the functions s_1' and s_2' with $r = 0.65$.

Then, the recovery of $\{f'(i_k)\}_{k=1}^n$ will be held by

$$(I - S_2')F' = S_1'F + h' \tag{3.4.5}$$

if $I - S_2'$ is invertible. The study of the invertibility of $I - S_2'$ is analogous to that of $I - S_1$. For $x \neq 0$,

$$\begin{aligned} x^H S_2' x &= \sum_m \sum_k s_2'(i_m - i_k) \\ &= \int_{-r}^{r} \widehat{s_2'} \underbrace{\left| \sum_k x_k e^{i2\pi\omega i_k} \right|^2}_{M(\omega)} d\omega. \end{aligned}$$

Recall that M is a periodic function with period of 1 Hz and note that

$$\begin{aligned} \widehat{s_2'} &= i\omega \hat{s_2} \\ &= i\omega(-i\text{sgn}(\omega)) \\ &= |\omega|. \end{aligned}$$

Then, similarly to S_1,

$$x^H S_2' x = \int_{-1/2}^{1/2} \left[|\omega - 1| \chi_{[1-r,-1/2]} + |\omega| + |\omega + 1| \chi_{[-1/2,r-1]} \right] M(\omega) d\omega.$$

Since $1/2 < r < 1$, there are at most two overlaps: $\widehat{s_2'}(\omega)$ either sums with $\widehat{s_2'}(\omega - 1)$ or with $\widehat{s_2'}(\omega + 1)$, but never with both simultaneously. Moreover, when the sums do occur, then

$$|\omega| + |\omega + 1| \chi_{[-1/2,r-1]} = 1$$

or

$$|\omega| + |\omega - 1| \chi_{[1-r,1/2]} = 1.$$

However, around zero there is a neighborhood where overlapping does not occur as can be seen in Figure 3.6. It then follows that

$$x^H S_2' x < \int_{-1/2}^{1/2} M(\omega) d\omega = \|x\|^2$$

and so $I - S_2'$ is invertible. Therefore, the recovery of missing samples of f' is also possible.

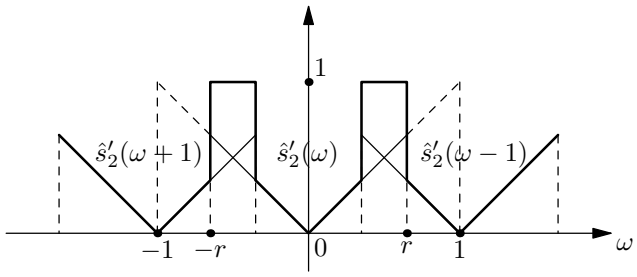

Figure 3.6: Spectral components of s_2'. The thick line corresponds to the sum of the components.

3.4.2.3 Missing Samples in Both Channels

A more delicate case is when samples of f and f' are unknown. The positions of the missing samples are now a subset of $\{f(i_k)\}_{k=1}^n \cup \{f'(i_k)\}_{k=1}^n$. Combining (3.4.4) and (3.4.5), one obtains the system

$$\underbrace{\begin{pmatrix} I - S_1 & -S_2 \\ -S_1' & I - S_2' \end{pmatrix}}_{S} \begin{pmatrix} F \\ F' \end{pmatrix} = \begin{pmatrix} h \\ h' \end{pmatrix}.$$

As above, recovery of the missing samples is only possible if S is invertible, where S is a $2n \times 2n$ matrix. But studying the invertibility of S has revealed to be a difficult task. Studying the kernel of S is equivalent to studying the invertibility of $I - (I - S_2')^{-1} S_1' (I - S_1)^{-1} S_2$ which is just as difficult. Other direct approaches lead to the same matrix, not solving nor simplifying the system. Turning to iterative approaches, the associated Gauss-Seidel method is given by

$$\begin{cases} x_{k+1} = S_1 x_k + S_2 y_k + h \\ \\ y_{k+1} = S_1' x_{k+1} + S_2' y_k + h' \end{cases}$$

and the associated matrix follows

$$G = \begin{pmatrix} S_1 & S_2 \\ S_1' S_1 & S_1' S_2 + S_2' \end{pmatrix}.$$

This method was favored because G can be factorized into

$$G = \underbrace{\begin{pmatrix} I & 0 \\ S_1' & I \end{pmatrix}}_{A} \underbrace{\begin{pmatrix} S_1 & S_2 \\ 0 & S_2' \end{pmatrix}}_{B}.$$

Moreover,

$$\begin{aligned} G - I &= \begin{pmatrix} S_1 - I & S_2 \\ S_1' S_1 & S_1' S_2 + S_2' - I \end{pmatrix} \\ &= \begin{pmatrix} I & 0 \\ S_1' & I \end{pmatrix} \begin{pmatrix} S_1 - I & S_2 \\ S_1' & S_2' - I \end{pmatrix} \\ &= A(-S). \end{aligned}$$

Then if 1 did not belong to the set of eigenvalues of G, S would be invertible. Although A has eigenvalues equal to 1 and $\rho(B) < 1$, where $\rho(B)$ denotes the spectral radius of B, $\rho(G) \leq \rho(A)\rho(B)$ is not true in general. Unfortunately, A and B do not satisfy commutation relations that could yield such inequality.

Note, however, that $I - S_1$ and $I - S_2'$ are symmetric whereas S_2 and S_1' are antisymmetric (duality of s_1 and s_2' and of s_1' and s_2). Numerical evidence shows that the number of occurrences of $\det(S) \neq 0$ is much more significant than otherwise. Although general sufficient conditions for $\det(S) \neq 0$ have not yet been established, more restrict conditions do exist via triangularization of the matrix. It, therefore, holds that $S_2 = 0$ if and only if $r(i_j - i_k) \in \mathbb{Z}$ for all $j, k \in \{1, ..., n\}$. As a result

$$\det(S) = \det(I - S_1) \det(I - S_2')$$

and from above it holds that $\det(S) \neq 0$. Moreover, $r(i_j - i_k) \in \mathbb{Z}$ for all $j, k \in \{1, ..., n\}$ if and only if there exist $p \in \mathbb{Z}$ and $q \in \mathbb{Z} \backslash \{0\}$ such that $\gcd(p, q) = 1$, $r = p/q$ (i.e., $r \in \mathbb{Q}$) and q is a common divisor of the set $\{i_j - i_k\}_{j,k=1}^{n}$. This means that the lost samples must be spaced (not necessarily in a consecutive manner) in a regular grid of distance q. Another possible result is that $S_1' = 0$ if and only if for all $j, k \in \{1, .., n\}$,

$$\cos(r(i_j - i_k)) = \operatorname{sinc}(r(i_j - i_k))$$

$$\cos(2r(i_j - i_k)) \;=\; \operatorname{sinc}(2r(i_j - i_k)).$$

In these conditions, it is also true that $\det(S) \neq 0$. Note, however, that for order > 2 it is not possible to have $S_2 = 0$ and $S_1' = 0$ simultaneously. It is interesting to observe that when samples are lost in only one channel, it is always possible to retrieve them. However, when the loss affects both channels, then recovery may not always be possible.

3.4.3 The Stability of the Recovery of Missing Samples

Even though the recovery of lost samples is possible in principle if certain invertibility conditions hold, in practice this may not suffice since there are finite precision limitations. Therefore, it is necessary that the system be also stable. Unstable systems lead to an exaggerated propagation in the output of a small perturbation in the input. This means that an approximation of a signal in an unstable system may result in huge discrepancies. Such stability can be measured via the condition number of the system. A low condition number indicates stability whereas a huge condition number indicates an ill-conditioned (or unstable) system. An ill-conditioned matrix can be seen, in practice, as a singular matrix (it is just as difficult to retrieve the signal f for an ill-conditioned system as it is for a singular system).

It has been mentioned that when $0 < r < 1/2$, the two-channel case resembles the single channel case. The stability of the reconstruction method for this case has already been studied [17]. Therefore r shall be taken to satisfy $1/2 < r < 1$.

When samples are lost in only one channel, the condition number of the system is relatively low for r around 0.5, growing abruptly as r approaches 1, as can be seen in Figure 3.7. This suggests that as r grows towards unity, the system loses stability becoming very ill-conditioned for $r \approx 1$. But when samples are lost in both channels, the system is generally ill-conditioned even if $r \ll 1$ as can be seen in Figure 3.7 (dotted line). This suggests that recovery of lost samples may not be feasible. An example that clearly illustrates this is that of Figure 3.8. The plot presents several peaks, one of which is situated at $r_1 = 0.596$. When r is slightly higher, $r_2 = 0.616$, the condition number lowers again. The effects of the peak and of the decrease in the condition number are depicted in Figure 3.9. Note how

the error norm for r_1 is much higher (for f as well as for f') than that of r_2 and how the system becomes greatly unstable for r_1 (the reconstructed version goes completely astray from the original signal). One may argue that since $r_1 < r_2$, then the stability for r_2 should be poorer, which is not the case. The point at r_1 represents a scenery of high instability (in spite of $r \ll 1$). Singularities (situations which yield $\det(S) = 0$) will also correspond to such peaks and the stability in the neighbourhood of the peaks will present a similar behaviour. This evidences the unexpected behaviour when samples are missing from both channels, even when $r \approx 0.5$, making reconstruction difficult in practice.

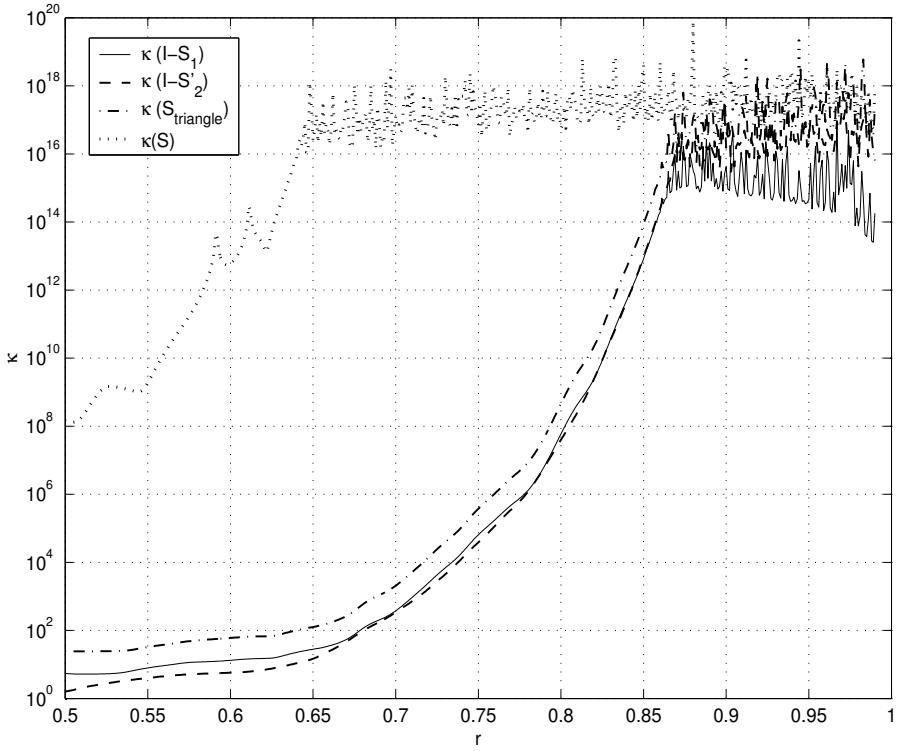

Figure 3.7: Log plot of the condition numbers for the different matrices, for a vector signal of size 50 and 20 erasures per channel. The curve corresponding to S_{triangle} refers to the block triangle matrix S with $S_2 = 0$.

When S is transformed into a triangular matrix ($S_2 = 0$ or $S_1' = 0$), then the condition number lowers dramatically for $r \ll 1$, peaking up as r approaches unity. In Figure 3.7 (dash-dotted curve corresponding to S_{triangle}), the plot is done for $S_2 = 0$. But for $S_1' = 0$ the plot is similar, since the case is analogous. This is the consequence that now the set of eigenvalues of S is reduced to $\sigma(S) = \sigma(I - S_1) \cup \sigma(I - S_2')$. Since $\rho(S_1), \rho(S_2') \ll 1$ when

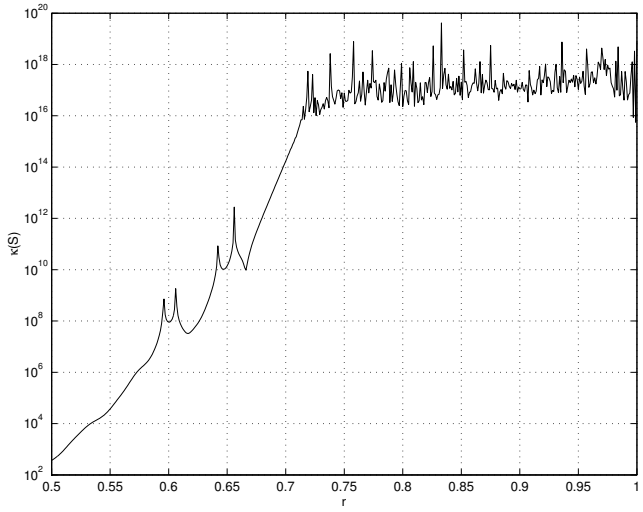

Figure 3.8: Log plot of the condition number in function of r, for a vector signal of size 50 and 20 erasures per channel at positions $X_1 = X_2 = \{1, 3, 5, 6, 9, 13, 22, 23, 26, 27, 29, 31, 32, 35, 37, 38, 41, 42, 44, 50\}$.

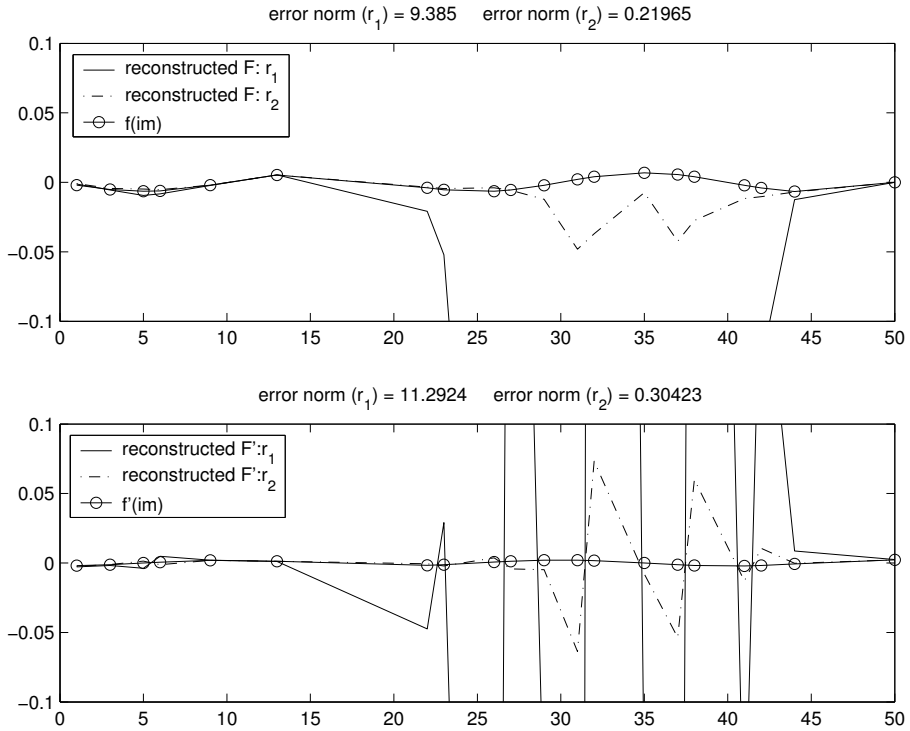

Figure 3.9: Representation of f (above: line with circles; the circles represent the missing samples) and of f' (bottom: line with circles), and their respective reconstruction versions for $r_1 = 0.596$ (solid line) and $r_2 = 0.616$ (dash-dotted line).

$r \ll 1$, the recovery of the lost samples is stable in this case. But when r approaches unity,

then $\rho(S_1), \rho(S_2') \approx 1$ yielding S ill-conditioned and jeopardizing the reconstruction.

Note that although r_0 must be rational to have $r_0(i_j - i_k) \in \mathbb{Z}$ for all $j, k \in \{1, ..., n\}$, due to the continuity of s_2 there exists $\varepsilon > 0$ such that for all $r \in (r_0 - \varepsilon, r_0 + \varepsilon)$, the system continues to be stable.

3.4.4 Infinite Number of Missing Samples

It is also of theoretical interest to study the reconstruction of the function and derivative system when an infinite number of samples is lost (as a limit case). Therefore, let $U = \{i_n\}_{n\in\mathbb{N}}$ denote the positions of such samples. Then analogously to the finite case, the recovery equation is given by

$$F = S_1 F + S_2 F' + h,$$

with the difference that the matrices and vectors involved are now of infinite dimension. It is further assumed that there exists $m \in \mathbb{N}$ such that $m > 1$ and m divides i_k, for all $k \in \mathbb{N}$ (for density convenience) [18].

When only function samples are lost, this is, when F' is known but F is not, F can be recovered as

$$(I - S_1)F = S_1 F' + h$$

if $I - S_1$ is invertible (much alike the finite case). To prove that indeed $I - S_1$ is invertible the arguments are analogous to those used in Section 3.4.2. Let $x \neq 0$. Then

$$\begin{aligned}
x^H S_1 x &= \sum_{k\in\mathbb{N}} \sum_{m\in\mathbb{N}} x_m^* x_k s_1(i_m - i_k) \\
&= \sum_{k\in\mathbb{N}} \sum_{m\in\mathbb{N}} x_m^* x_k \int_{-r}^{r} \hat{s}_1(\omega) e^{i2\pi\omega(i_m - i_k)} d\omega \\
&= \int_{-r}^{r} \hat{s}_1(\omega) \sum_{k\in\mathbb{N}} \sum_{m\in\mathbb{N}} x_m^* x_k e^{i2\pi\omega(i_m - i_k)} d\omega \qquad \text{(convergent series in } L^2\text{)} \\
&= \int_{-r}^{r} \hat{s}_1(\omega) \underbrace{\left| \sum_{k\in\mathbb{N}} x_k e^{i2\pi\omega i_k} \right|^2}_{M(\omega)} d\omega.
\end{aligned}$$

As with the finite case,

$$\begin{aligned} x^H S_1 x &= \int_{-r}^{-1/2} \hat{s}_1(\omega) M(\omega) d\omega + \int_{-1/2}^{1/2} \hat{s}_1(\omega) M(\omega) d\omega + \int_{1/2}^{r} \hat{s}_1(\omega) M(\omega) d\omega \\ &= \int_{-1/2}^{1/2} \hat{s}_1(\omega - 1) \chi_{[1-r,1/2]} M(\omega - 1) d\omega + \int_{-1/2}^{1/2} \hat{s}_1(\omega) M(\omega) d\omega + \\ &\quad \int_{-1/2}^{1/2} \hat{s}_1(\omega + 1) \chi_{[-1/2,r-1]} M(\omega + 1) d\omega. \end{aligned}$$

From the existence of $m > 1$ which divides all i_k, it follows that M is a periodic function with period $1/m$. Then

$$\int_{-1/2}^{1/2} M(\omega) d\omega = m \int_{-1/2m}^{1/2m} M(\omega) d\omega,$$

that is, M is periodic (with m cycles) in $[-1/2, 1/2]$. It follows that

$$x^H S_1 x = \int_{-1/2}^{1/2} \left(\hat{s}_1(\omega - 1) \chi_{[1-r,1/2]} + \hat{s}_1(\omega) + \hat{s}_1(\omega + 1) \chi_{[-1/2,r-1]} \right) M(\omega) d\omega.$$

Since $1/2 < r < 1$ the overlapping arguments used for the finite case are valid. Thus,

$$\hat{s}_1(\omega) = 1 - |\omega|, \quad \omega \in [-r, r]$$

and so the overlapping regions sum as

$$\hat{s}_1(\omega - 1) + \hat{s}_1(\omega) = \hat{s}_1(\omega) + \hat{s}_1(\omega + 1) = 1.$$

Moreover, there are regions where overlap of components does not occur (Figure 3.4). Under these considerations,

$$x^H S_1 x < \int_{-1/2}^{1/2} M(\omega) d\omega = m \int_{-1/2m}^{1/2m} M(\omega) d\omega = m \frac{\|x\|^2}{m} = \|x\|^2.$$

Thus, $\rho(S_1) < 1$ and hence $I - S_1$ is invertible. It is then possible to recover F. An iterative approach to obtain F (which also holds for the finite case) can be given by

$$F_{n+1} = S_1 F_n + c,$$

where $c = S_2F' + h$. Since $\rho(S_1) < 1$, the method converges.

When in turn only derivative samples are lost, i.e., F is known but F' is unknown, then F' can be recovered by

$$F' = S_1'F + S_2'F' + h'$$

as

$$(I - S_2')F' = S_1'F + h'$$

if $I - S_2'$ is invertible. Indeed analogously to S_1, let $x \neq 0$. Then

$$x^H S_2' x = \int_{-r}^{r} \widehat{s_2'}(\omega) \underbrace{\left| \sum_{k\in\mathbb{N}} e^{i2\pi\omega i_k} \right|^2}_{M(\omega)} d\omega.$$

Because M is a periodic function with m cycles in $[-1/2, 1/2]$, it holds that

$$x^H S_2' x \;=\; \int_{-1/2}^{-1/2} \left(\widehat{s_2'}(\omega - 1)\chi_{[1-r,1/2]} + \widehat{s_2'}(\omega) + \widehat{s_2'}(\omega + 1)\chi_{[-1/2,r-1]} \right) M(\omega) d\omega.$$

Since $1/2 < r < 1$ then at most two components of $\widehat{s_2'}$ overlap, existing a region around $\widehat{s_2'}(\omega)$ where overlapping is absent. Moreover,

$$\widehat{s_2'}(\omega) = |\omega|, \quad \omega \in [-r, r]$$

and so the overlapping regions sum up as 1. Hence

$$x^H S_2' x < \int_{-1/2}^{-1/2} M(\omega) d\omega = m \int_{-1/2m}^{1/2m} M(\omega) d\omega = m \frac{\|x\|^2}{m} = \|x\|^2.$$

Then $\rho(S_2') < 1$ and so $I - S_2'$ is invertible. Therefore, it is also possible to recover F'. Iteratively, F' can be obtained by

$$F'_{n+1} = S_2' F'_n + c,$$

where $c = S_1'F + h'$. Since $\rho(S_2') < 1$, the method converges.

When both function and derivative samples are lost, the system is not so well-behaved. As for the finite case, the system to reconstruct F and F' is given by

$$\underbrace{\begin{pmatrix} I - S_1 & -S_2 \\ -S_1' & I - S_2' \end{pmatrix}}_{S} \begin{pmatrix} F \\ F' \end{pmatrix} = \begin{pmatrix} h \\ h' \end{pmatrix}$$

where the matrices and vectors involved are of infinite dimension. It has been observed that a sufficient condition for S to be invertible is to have $S_2 = 0$. Moreover, $S_2 = 0$ if and only if $r(i_j - i_k) \in \mathbb{Z}$, for all $j, k \in \mathbb{N}$, which is equivalent to the existence of $p \in \mathbb{Z}$ and $q \in \mathbb{Z}\backslash\{0\}$ such that $\gcd(p, q) = 1$, $r = p/q$ and q divides $\{i_j - i_k\}_{j,k\in\mathbb{N}}$. Obviously, if r is irrational, then $S_2 \neq 0$. An immediate corollary taking into account the existence of m, is that, if $rm \in \mathbb{N}$ which is equivalent to q divides m then $S_2 = 0$. Note, however, that this is only a sufficient condition for $S_2 = 0$. An iterative method to obtain F and F' could be

$$\begin{cases} F_{n+1} = S_1 F_n + S_2 F_n' + h \\ F_{n+1}' = S_1' F_{n+1} + S_2' F_n' + h', \end{cases} \tag{3.4.6}$$

but this method will not always converge, since $\det S$ can be zero, i.e., reconstruction may not always be possible.

3.5 The Function and Delayed Derivative Case

When a two-channel system is unstable, it is usual to introduce a delay in one set of samples. This approach can help simplify the problem and even improve stability. But this method is not always successful. Since the function and derivative system is generally ill-conditioned, we consider a delay in the derivative samples (a delay in the function samples is analogous).

Therefore consider samples of f and samples of f' with a delay δ associated to them. The reconstruction series now becomes (details in Appendix B),

$$f(t) = \sum_{k=-\infty}^{\infty} (f(k)s_1(t-k) + f'(k)s_2(t-k))$$

where

$$\hat{s}_1(\omega) = \frac{\sqrt{2\pi}}{b}\frac{1+\omega/b}{1+c_1\omega/b}, \quad \omega \in [-\omega_a, 0]$$

$$\hat{s}_1(\omega) = \frac{\sqrt{2\pi}}{b}\frac{1-\omega/b}{1-a_1\omega/b}, \quad \omega \in [0, \omega_a]$$

with $a_1 = 1 - e^{-i\delta\omega_s}$, $b = \omega_s$, $c_1 = 1 - e^{i\delta\omega_s}$ and

$$\hat{s}_2(\omega) = \frac{\sqrt{2\pi}i}{b}\frac{1}{(\omega a_2 + b a_2 - \omega)e^{-i\delta\omega}}, \quad \omega \in [-\omega_a, 0]$$

$$\hat{s}_2(\omega) = \frac{\sqrt{2\pi}i}{b}\frac{1}{(\omega c_2 - b c_2 - \omega)e^{-i\delta\omega}}, \quad \omega \in [0, \omega_a]$$

with $a_2 = e^{-i\delta\omega_s}$ and $c_2 = e^{i\delta\omega_s}$. The integration of these terms to obtain s_1 and s_2 do not lead to analytic solutions. Expanding $\hat{s}_1$ and $\hat{s}_2$ one obtains

$$\hat{s}_1(\omega) = \frac{\sqrt{2\pi}}{b}\left(1 + \frac{c_1 - 1}{c_1}\sum_{n=1}^{\infty}\left(-\frac{c_1\omega}{b}\right)^n\right), \quad \omega \in [-\omega_a, 0]$$

$$\hat{s}_1(\omega) = \frac{\sqrt{2\pi}}{b}\left(1 + \frac{a_1 - 1}{a_1}\sum_{n=1}^{\infty}\left(\frac{a_1\omega}{b}\right)^n\right), \quad \omega \in [0, \omega_a]$$

and

$$\hat{s}_2(\omega) = \frac{\sqrt{2\pi}i}{b^2 a_2}\sum_{n=0}^{\infty}(-1)^n\frac{(a_2-1)^n}{b^n a_2^n}\omega^n, \quad \omega \in [-\omega_a, 0],$$

$$\hat{s}_2(\omega) = -\frac{\sqrt{2\pi}i}{b^2 c_2}\sum_{n=0}^{\infty}\frac{(c_2-1)^n}{b^n c_2^n}\omega^n, \quad \omega \in [0, \omega_a].$$

When $\delta < 1/6$, convergence is guaranteed and, thus, s_1 and s_2 exist in this case (details in Appendix B). It then follows for $\delta < 1/6$ that

$$s_1(t) = -\frac{1}{b}D(0, -\omega_a) - \frac{1}{b}\frac{c_1 - 1}{c_1}\sum_{n=1}^{\infty}\left(-\frac{c_1}{b}\right)^n D(n, -\omega_a) + \frac{1}{b}D(0, \omega_a) +$$

$$\frac{1}{b}\frac{a_1 - 1}{a_1}\sum_{n=1}^{\infty}\left(\frac{a_1}{b}\right)^n D(n, \omega_a)$$

and

$$s_2(t) = -\frac{i}{b}\sum_{n=0}^{\infty}(-1)^n\frac{(a_2-1)^n}{b^{n+1}a_2^{n+1}}D(n,-\omega_a) - \frac{i}{b}\sum_{n=0}^{\infty}\frac{(c_2-1)^n}{b^{n+1}c_2^{n+1}}D(n,\omega_a)$$

where

$$D(n,\gamma) = \int_0^{\gamma}\omega^n e^{i\omega t}d\omega.$$

It is quite obvious that the delay introduced in this case did not simplify the problem but complicated it dramatically.

3.6 Generalizations due to Kim and Kwon

The results presented in [26] follow the line of thought of our results in [40, 41] and generalize the latter for filter banks with two arbitrary channels (Figure 3.1). For the sake of completeness and because of their interest, they are discussed here.

3.6.1 The Oversampled Expansion

Consider a signal f bandlimited to r Hz ($\mathrm{supp}(\hat{f}) \in [-r,r]$) where $1/2 < r < 1$. Furthermore, consider a two-channel filter bank such that its analysis filters h_1 and h_2 satisfy $|\det a(w)| \geq \alpha$ a.e. with $w \in [-1,0]$, where $\alpha > 0$ and

$$a(w) = \begin{pmatrix} h_1(w) & h_1(w+1) \\ h_2(w) & h_2(w+1) \end{pmatrix}$$

is the transfer matrix. Let $c_1(f), c_2(f)$ be the outputs of the system.

Since f is bandlimited, then f can be expressed as a critical sampling expansion of its samples [24, 33],

$$f(t) = \sum_k c_1(f)(k)s_{1k}(t) + c_2(f)(k)s_{2k}(t) \tag{3.6.1}$$

where $\{s_{jk}\}$ is a Riesz basis for the space of functions bandlimited to r Hz. It follows that $\{\phi_{jk}\}$, where $\phi_{jk} = \widehat{s}_{jk}$, is a Riesz basis for $L^2[-r,r]$.

Let η be a bounded measurable function on $[-1,1]$ such that $\eta(w)=1$ on $[-r,r]$. Then it is possible to write an oversampling expansion series as [26] (cf. (3.3.1)),

$$f(t)=\sum_k c_1(f)(k)T_{1k}(t)+c_2(f)(k)T_{2k}(t) \tag{3.6.2}$$

where

$$T_{jk}(t)=\int_{-1}^{1}\phi_{jk}(w)\eta(w)e^{i2\pi tw}dw, \quad j=1,2.$$

3.6.2 Reconstruction with Missing Samples

Critical sampling (3.6.1) is sufficient to reconstruct f, but it cannot reconstruct the signal when samples are lost. In this case, as mentioned in Section 3.2, oversampling is necessary (3.6.2), although reconstruction is not always guaranteed.

Consider $U_1=\{m_{11},...,m_{1M}\}$ to be the set of the positions of lost samples in the first channel, $U_2=\{m_{21},...,m_{2N}\}$ the set of the positions of lost samples in the second channel and $U=U_1\cup U_2$. Then from (3.6.2), it is possible to express the missing samples as a linear combination of the rest of the samples,

$$\begin{aligned} c_l(f)(m) &= \sum_k\sum_{j=1}^{2} c_j(f)(k)\left\langle \phi_{j,k}h,\phi^*_{l,m}\right\rangle \\ &= \sum_k\sum_{j=1}^{2} c_j(f)(k)R_{l,j}(m,k) \\ &= \sum_{k\in U}\sum_{j=1}^{2} c_j(f)(k)R_{l,j}(m,k)+h(m), \quad l=1,2 \end{aligned} \tag{3.6.3}$$

where

$$h(m) = \sum_{k\notin U}\sum_{j=1}^{2} c_j(f)(k)R_{l,j}(m,k), \quad m\in U,$$

is the component corresponding to the known samples. In matricial notation, (3.6.3) becomes

$$\begin{pmatrix} F_1 \\ F_2 \end{pmatrix} = \begin{pmatrix} S_{11} & S_{12} \\ S_{21} & S_{22} \end{pmatrix} \begin{pmatrix} F_1 \\ F_2 \end{pmatrix} + h$$

or

$$F = SF + h \tag{3.6.4}$$

where $F = (\, F_1 \quad F_2 \,)^T$ and

$$F_1 = \begin{pmatrix} c_1(f)(m_{11}) \\ \vdots \\ c_1(f)(m_{1M}) \end{pmatrix}^T \qquad F_2 = \begin{pmatrix} c_2(f)(m_{21}) \\ \vdots \\ c_2(f)(m_{2N}) \end{pmatrix}^T .$$

Furthermore,

$$S = \begin{pmatrix} S_{11} & S_{12} \\ S_{21} & S_{22} \end{pmatrix}$$

with

$$\begin{aligned} S_{11} &= (\, R_{11}(m_{1i}, m_{1j}) \,)_{i,j=1}^{M} \\ S_{12} &= (\, R_{12}(m_{1i}, m_{2j}) \,)_{i=1,j=1}^{M \quad N} \\ S_{21} &= (\, R_{21}(m_{2i}, m_{1j}) \,)_{i=1,j=1}^{N \quad M} \\ S_{22} &= (\, R_{22}(m_{2i}, m_{2j}) \,)_{i,j=1}^{N} \end{aligned}$$

and $h = (\, h(m) \,)_{m \in U}$. The recovery of the missing samples is possible if it is possible to solve the system given by (3.6.4).

Consider, at first, that the missing samples belong to the first channel and that all samples from $c_2(f)$ are known ($U_2 = \emptyset$). Then (3.6.4) is reduced to

$$F_1 = S_{11} F_1 + h,$$

or equivalently

$$(I - S_{11})F_1 = h.$$

If $I-S_{11}$ is invertible, then F_1 can be recovered. This means that if $I-S_{11}$ is invertible, then the missing samples from $c_1(f)$ are recovered and, hence, the signal can be reconstructed. Let

$$\begin{aligned} E_1 &= \{w \in [-1, -r] : h_1(w)h_2(w+1) \neq 0\} \\ E_2 &= \{w \in [-(1-r), 0] : h_1(w+1)h_2(w) \neq 0\} \end{aligned}$$

and $E = E_1 \cup E_2$. It is shown in [26] that if $|E| > 0$ (where $|E|$ denotes the Lesbesgue measure[1] of E), then $I - S_{11}$ is invertible.

In turn, when samples are missing from the second channel only ($U_1 = \emptyset$), the situation is analogous. The system (3.6.4) reduces to

$$F_2 = S_{22}F_2 + h$$

which is equivalent to

$$(I - S_{22})F_2 = h.$$

If $I-S_{22}$ is invertible, then F_2 can be recovered and, in this case, the missing samples from $c_2(f)$ can be recovered. Similarly as done above, let

$$\begin{aligned} E_1 &= \{w \in [-1, -r] : h_1(w+1)h_2(w) \neq 0\} \\ E_2 &= \{w \in [-(1-r), 0] : h_1(w)h_2(w+1) \neq 0\} \end{aligned}$$

and $E = E_1 \cup E_2$. It is shown in [26] that if $|E| > 0$, then $I - S_{22}$ is invertible.

For the case when sample loss affects both channels, the situation is more complicated as confirmed for the function and derivative case. Let $\eta = \chi_{[-r,r]}$ and consider the orthogonal projection P given by

$$\begin{aligned} P : L^2[-1, 1] &\rightarrow L^2[-r, r] \\ \varphi &\mapsto h\varphi. \end{aligned}$$

[1]The Lesbesgue measure is an extension of the standard measure in euclidean spaces. In our case, it is exactly the standard measure of length of the respective intervals, i.e., the amplitude of the intervals.

Moreover, let $B_+ = [0, r]$ and $B_- = [-r, 0]$ denote the positive and negative side of the signal's band. Recall that $\{\phi_{jk}\}$ is a Riesz basis for $L^2[-r, r]$. Then there exists an orthonormal base $\{e_{jk}\}$ and a bounded invertible operator T such that $\phi_{jk}(w) = (T^*)^{-1}(e_{jk}(w))$.

Two sufficient conditions where presented in [26] which guarantee the recovery of the missing samples from both channels:

> Theorem 1: Suppose that $PT = TP$. Then F is recovered if and only if $|B_+| < 1$ and $|B_-| < 1$.
>
> Theorem 2: Assume $|B_\pm| < 1$. Then F is recovered if one of the three conditions is satisfied
>
> 1. $B_+ = B_- - 1$
> 2. $\begin{cases} a_1(w) = 0, & w \in [0, 1-r] \cup [r, 1] \\ a_2(w) = 0, & w \in [-1, -r] \cup [-1+r, 0] \end{cases}$
> 3. $\begin{cases} a_1(w) = 0, & w \in [-1, -r] \cup [-1+r, 0] \\ a_2(w) = 0, & w \in [0, 1-r] \cup [r, 1]. \end{cases}$

The results presented in Section 3.4 are in accordance with these generalizations.

3.7 Conclusion

In the single channel (classical) sampling theorem, any finite number of missing samples can always be recovered. The stability of the procedure is well-known to depend on r. More precisely, as r tends to unity, the system becomes ill-conditioned, jeopardizing the reconstruction in practice. In the two-channel sampling case, the recovery of missing samples is much more delicate.

The oversampled series expansion for function and derivative sampling was established, in order to study the recovery of lost samples that can occur in only one channel or in both channels. When the oversampling parameter is such that $r < 1/2$, the two-channel filter bank resembles the single channel case for which both reconstruction and stability have been studied [16, 17]. In turn, when $r \geq 1/2$ the system is oversampled whereas

each channel is undersampled in the presence of erasures, making samples of both channels necessary for the reconstruction of the signal f.

Samples lost in only one channel can always be recovered. In this case, the reconstruction algorithm is simple and efficient: the reconstruction of n lost samples in one of the two channels can be performed by solving a set of n linear equations. As in the classical case, when r tends to unity the system becomes so unstable (the system matrix becomes ill-conditioned) that in practice recovery may not be feasible.

In turn, when sample loss affects both channels, the system matrix is usually invertible but ill-conditioned (there are many more occurrences of $\det S \neq 0$ than otherwise; moreover, there are many more occurrences of large condition numbers than otherwise). This means that although the recovery of lost samples is usually possible in principle, the system is usually ill-conditioned and, thus, the recovery may not be feasible in practice. It is as difficult to recover a signal for an ill-conditioned system as it is for a singular one. Occurrences of singular S exist and recovery of samples, in this case, is impossible even in principle. Nevertheless for the particular case when one of the blocks S_2 or S_1' is zero, the stability of the system is dramatically improved (for $r \ll 1$), since the eigenvalues now involved belong only to $I - S_1$ and $I - S_2'$. In fact, the stability in this case depends only on r: as r approaches unity, the matrix condition number explodes; when r is away from unity the system is reasonably stable and the recovery of the missing samples is feasible.

As for the theoretical interest in the recovery of an infinite number of missing samples, the arguments used to prove that reconstruction is possible for samples lost in only one of the channels are very similar to those used for the finite case. The sufficient condition that guarantees reconstruction when sample loss affects both channels is also analogous to the finite situation and the iterative methods presented in Section 3.4.4 are also valid for the finite case (Section 3.4.2). Moreover, the iterative method given by (3.4.4) may not always converge, since reconstruction may not always be possible.

In general, the matrix S has revealed difficult to study. Clearly the eigenvalues of S do not only depend on r, in general, since for $r \ll 1$ ill-conditioning is usually present (dotted line in Figure 3.7). Even introducing a delay, δ, in one set of samples does not simplify

the system. On the contrary, it is interesting to observe that the delayed system is much more complex than the previous one and that the integrals associated to s_1 and s_2 do not have an analytic expression. Moreover, convergence of the associated series (the existence of s_1 and s_2) is only guaranteed for $\delta < 1/6$.

Generalizations of the above results were presented in [26]. When the two channels are arbitrary, the reconstruction of the signal is jeopardized even if sample loss affects only one channel. The assumption that the transfer matrix satisfies $|\det a(w)| \geq \alpha$ guarantees stability conditions. Without these conditions, the results presented in Section 3.6 would not be valid.

Note that when samples are missing from only one channel, the reconstruction of f depends strongly on the analysis filters. Applying these results to the functional and derivative case, $h_1(w) = 1$ e $h_2(w) = iw$ with $c_1(f) = f$ e $c_2(f) = f'$. For samples lost in the first channel, the sets E_1 and E_2 become

$$\begin{aligned} E_1 &= \{w \in [-1, -r] : i(w+1) \neq 0\} =]-1, -r] \\ E_2 &= \{w \in [-1+r, 0] : iw \neq 0\} = [-1+r, 0[\end{aligned}$$

and for samples lost in the second channel

$$\begin{aligned} E_1 &= \{w \in [-1, -r] : iw \neq 0\} = [-1, -r] \\ E_2 &= \{w \in [-1+r, 0] : i(w+1) \neq 0\} = [-1+r, 0]. \end{aligned}$$

Since $r < 1$, it follows that $|E| = |E_1 \cup E_2| > 0$. Hence the signal can always be reconstructed, which is in accordance with the results presented in Section 3.4. However, when samples are lost from both channels, the signal cannot always be recovered in the functional and derivative filter bank. This is confirmed by Theorem 2, since $|B_{\pm}| < 1$ (because $r < 1$) and none of the three conditions are satisfied.

Chapter 4

Error Locator Polynomial and DNA Sequences

4.1 Introduction

It this chapter, the subject that is focused is the redundancy present in DNA sequences. Apparently it may seem that there is no connection with the previous chapters, but redundancy is also studied here and this redundancy can be used to error-check and reconstruct DNA sequences.

DNA and protein sequences can be represented by character strings from an alphabet of four letters and 20 letters, respectively. In the case of DNA sequences, these can be written as strings of symbols, $s = s_0...s_{n-1}$, where $s_i \in \{A, C, G, T\}$ (for $i = 0, ..., n-1$). The set $\{A, C, G, T\}$ is the alphabet and the choice of such an alphabet is motivated by the fact that DNA sequences consist of four nucleotides: adenine (A), cytosine(C), guanine (G) and thymine (T). This alphabet is useful in methods for detecting and revealing structure (short and long range correlations, periodicities, and so on) in the DNA sequence after a convenient numerical transformation. These methods then provide information that can help identify functional regions and other underlying structures.

In particular, several periodicities exist within DNA sequences which reveal certain structures. The most important of these are the 3-periodicity (related to coding regions) and the 10-11-periodicity (related to coiling of the DNA molecule). Many methodologies have been used to look into these underlying periodicities and other structures, such as

short and long range correlations, among which Fourier or linear transform analysis present themselves as natural tools for such a task. An overview of the several methods can be found in [1]. A convenient numerical treatment of the sequence must however be employed in order to avoid apparent structures that are inherent to the symbol-to-number mapping used and not to the sequence itself. For example, consider the sequence given by $s = ACGTACGTACGTACGT$ and three different mappings,

$$\begin{aligned} f_1(A) &= 1 \quad f_1(C) = 2 \quad f_1(G) = 4 \quad f_1(T) = 3 \\ f_2(A) &= 1 \quad f_2(C) = 3 \quad f_2(G) = 2 \quad f_2(T) = 4 \\ f_3(A) &= 1 \quad f_3(C) = 4 \quad f_3(G) = 3 \quad f_3(T) = 2 \end{aligned}$$

The spectrum of the mappings is shown in Figure 4.1. Note that the periods are different for each mapping revealing that the periodicities present are due to the mappings and not to the sequence. This is undesirable since it is misleading.

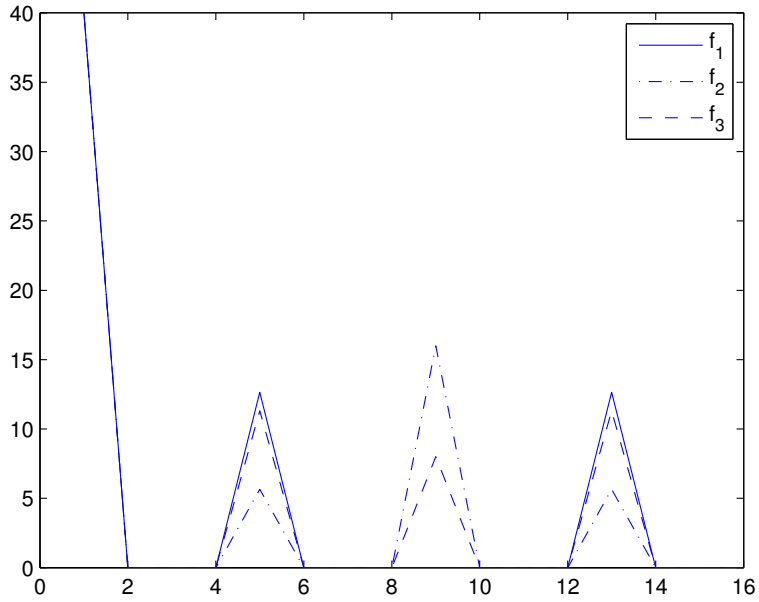

Figure 4.1: Spectrum of mappings f_1, f_2 and f_3.

This problem can be circumvented by considering the indicator sequences of s, that is, the indicator functions for each nucleotide, i_A, i_C, i_G and i_T. This is a very simple choice

which only takes into consideration the fact that A, C, G and T are distinct; no other assumption is made. From these indicator sequences, one obtains the spectral components, $I_A(k)$, $I_C(k)$, $I_G(k)$ and $I_T(k)$, as well as the spectrum of the sequence $S(k)$ (for $k = 0, ..., n-1$) by Fourier analysis. The spectral coefficients of the sequence carry important information about the structures and periodicities present in the sequence. For example, the connection between the distribution of the nucleotides in the sequence, at certain positions, and the magnitude of the spectral coefficients $S(k)$ has already been noticed [27]. One of the most important of these components is $S(n/3)$ which is related to 3-periodicity, since it can help to identify protein coding regions from non-coding ones. Two other important ones are $S(n/10)$ and $S(n/11)$ which are related to 10-11-periodicity which in turn is related to the coiling of DNA.

The redundancy present in the spectral components of each indicator sequence was found to be described by a special linear recursion, called the error-locating polynomial. In the context of error-correcting codes, the error-locating polynomial is well-known [19, 46] and was discussed in Section 2.2.2. Recall that this polynomial satisfies

$$P(i_p) = \sum_{k=0}^{m} h_k e^{j2\pi k i_p/n} = 0, \quad p = 0, ..., m-1, \tag{4.1.1}$$

where $i_0, ..., i_{m-1}$ are the positions of the missing samples of a bandlimited signal x with n samples and such that $h_m = 1$. The positions of the missing samples are determined by the polynomial zeros (4.1.1). It can be shown using this polynomial that for DNA sequences, the spectral components are redundant. More precisely, for m occurrences of a symbol B in a sequence of length n, the n spectral components associated to B can be determined from any contiguous set of occurrences of cardinal m by means of a linear recursion that involves the polynomial (4.1.1). The application of the error locator polynomial to DNA sequences (among other results) gave rise to the article [2].

4.2 Indicator Sequences

Let $s = s_0...s_{n-1}$ be a symbolic sequence with elements pertaining to the alphabet $\{A, C, G, T\}$ and associated to a certain DNA sequence. Then the indicator sequence for the symbol $B \in \{A, C, G, T\}$ with respect to the symbolic sequence s is given by

$$i_B(j) = \begin{cases} 1, & s_j = B, \\ 0, & \text{otherwise}, \end{cases}$$

with $j = 0, ..., n-1$. Note that the binary sequence i_B indicates the positions of the base B in the sequence s by assigning 1 to those positions. Since there are four nucleotides, there are four indicator sequences: i_A, i_C, i_G and i_T. Moreover note that the sequence 1...1 (all ones) is obtained by adding the four indicator sequences together, i.e., the indicator sequences are redundant since three are sufficient to determine the symbolic sequence. The Fourier spectrum of the sequence s (extension modulo n is assumed whenever necessary: $s_{n+k} = s_k$) is defined in terms of the four individual spectra of the indicator sequences [3, 49, 50]. More precisely, the n Fourier coefficients $S(k)$ $(0 \leq k < n)$ are given by

$$S(k) = |I_A(k)|^2 + |I_C(k)|^2 + |I_G(k)|^2 + |I_T(k)|^2, \tag{4.2.1}$$

where I_A, I_C, I_G and I_T are the discrete Fourier transforms (DFT) of the indicator sequences, that is,

$$I_B(k) = \sum_{j=0}^{n-1} i_B(j) e^{-i2\pi jk/n} \tag{4.2.2}$$

where B is one of the four symbols A, C, G, T (the i in the exponent denotes the imaginary unit and not j as in previous sections). Note that for convenience the Fourier transform used here is not the one used in Chapter 2. Here the inverse is therefore given by

$$i_B(j) = \frac{1}{N} \sum_{k=0}^{n-1} I_B(k) e^{i2\pi kj/n}.$$

The sequences $I_A(k)$, $I_C(k)$, $I_G(k)$ and $I_T(k)$ provide a four-dimensional representation of the frequency spectrum of the string. Note, however, that since the indicator sequences

are redundant, then $I_A(k)$, $I_C(k)$, $I_G(k)$ and $I_T(k)$ are also redundant. Moreover, since the indicator sequences always add up to 1, then

$$I_A(k) + I_C(k) + I_G(k) + I_T(k) = \begin{cases} N, & k = 0 \\ 0, & k \neq 0 \end{cases}.$$

In turn, $S(k)$ combines the contributions of all four characters and has been used as a measure of the total spectral content of the DNA string at frequency k [1]. Moreover, it harbors the desired invariance properties mentioned above. $S(k)$ is useful for finding periodicities in the DNA sequence. For example, the frequency at $k = n/3$ corresponds to a period of three nucleotides (short-range correlations) which is the length of each triplet in the sequence (also known as codons). It is known that the spectrum of protein coding DNA typically has a peak at that frequency [3]. Other periodicities are also important, such as that of $S(n/10)$ and $S(n/11)$.

Periodicities correspond to peaks in the spectrum plot. These peaks indicate the location of potential structures but do not indicate which symbols are involved in the periodic structure. Furthermore, multiple peaks do not indicate that several components have been added but that components interleave, which means that some spectral components cannot occur (periods that are mutually prime). When periodicities do occur, the symbols involved can be determined by an optimizes version of $S(k)$.

This optimized version of $S(k)$ is given by $|aI_A + cI_C + gI_G + tI_T|^2$ where a, c, g, t are adequately chosen constants [1]. The constants are adjusted in such a way that the spectral energy of the spectrum is maximized, i.e., for $w = (\,a \quad c \quad g \quad t\,)^T$ and $U = (\,I_A \quad I_C \quad I_G \quad I_T\,)^T$ the constants a, c, g, t are solutions to the optimization problem given by

$$\max_{\|w\|=1} \quad w^H U^H U w.$$

Hence, the values of a, c, g, t weigh the contributions of each symbol for the underlying structures. However, this result is much more difficult to compute than (4.2.1).

4.3 The Error Locator Polynomial

In this section, the error-locating polynomial (discussed in section 2.2.2) is revisited in order to adjust the notation to this particular chapter. It will be treated here still in the context of error-correcting codes. The migration to DNA sequences is treated in the next section.

Assume x to be a bandlimited signal and $\{x_k\}_{k=0}^{n-1}$ the set of samples from which x can be reconstructed (with oversampling). Assume moreover that $U = \{i_0, ..., i_{m-1}\}$ is the set of the positions of m errors occurring in $\{x_k\}$. The set U is unknown (nonlinear problem) and the objective is to determine it, thus, reducing U to the set of erasures (errors with known positions) occurring in x_k (linear problem).

Consider the error locator polynomial given by

$$P(z) = \sum_{l=0}^{m} h_l z^l \tag{4.3.1}$$

with $h_m = 1$ (normalization condition) and

$$P(e^{-i2\pi i_p/n}) = 0, \quad 0 \leq p < m.$$

The coefficients of $P(z)$ can be determined from the observed data $\{x_k\}_{k \notin U}$ (cf. section 2.2.2), and so the position of the m errors follows from the m roots of $P(z) = 0$ as the coefficients of the recursion (4.3.1).

4.4 Redundancy in the DNA Spectrum

In this section, it will be shown how the polynomial (4.2.1) can be applied in the context of DNA spectral components.

The spectral coefficients of a symbolic sequence are not independent. To show this, consider the indicator sequence i_B for $B \in \{A, C, G, T\}$ and its DFT I_B. Let i_B have length n with m ones, located at $U = \{j_0, j_1, \ldots, j_{m-1}\}$. Then $i_B(j) = 1$ if and only if

$j \in U$. The n spectral coefficients of I_B given by (4.2.2) satisfy the recursion

$$I_B(\ell + m) = -\sum_{k=0}^{m-1} h_k I_B(\ell + k), \tag{4.4.1}$$

where h_k are the coefficients of the error locator polynomial (4.3.1). To prove this statement consider the m equations given by

$$P\left(e^{-i2\pi j_p/n}\right) = \sum_{k=0}^{m} h_k e^{-i2\pi j_p k/n} = 0, \qquad 0 \le p < m$$

which results from the substitution of z in the polynomial by each of its roots $z = e^{-i2\pi j_p k/n}$. Multiplication of each of them by

$$i_B(j_p) e^{-i2\pi j_p \ell/n},$$

followed by summation over p and an interchange of the summation order yields

$$\sum_{k=0}^{m} h_k \sum_{p=0}^{m-1} i_B(j_p) e^{-i2\pi j_p(\ell+k)/n} = \sum_{k=0}^{m} h_k \sum_{p=0}^{n-1} i_B(p) e^{-i2\pi p(\ell+k)/n}.$$

Combination with (4.2.2) gives a relation between the spectral components of B,

$$\sum_{k=0}^{m} h_k I_B(\ell + k) = 0,$$

and since $h_m = 1$ we finally get the result. Equation (4.4.1) shows that there is redundancy in the spectral components of the sequence. Moreover, it shows that any set of m consecutive coefficients determine the remaining $n - m$ coefficients. Note that the polynomial describes the redundancy in the components in such a way that prediction of subsequent components can be made or sequences that have been predicted can be checked for errors via their spectral components.

4.5 Conclusion

Writing DNA sequences as strings of symbols has the advantage that with the convenient numerical transform, one can investigate underlying correlations. The symbol-to-number mapping must be label invariant, since structures that are not inherent to sequence but to the mapping are misleading. The underlying structures and correlations include periodicities which seem natural to exploit by means of Fourier analysis. Moreover, Fourier analysis has the advantage of being flexible. Hence, the concept of indicator sequence was introduced. These sequences provide a simple and general numerical treatment of the sequence (the only assumption made is that the symbols A, C, G and T are distinct). By taking the DFT of each sequence, the spectral components of each indicator sequence are obtained. The total spectrum is given by the sum of the squared modulus of the components and exhibits the desired label invariance. However, when using Fourier analysis periodicity modulo n (size of the symbolic sequence) is implied. Strong periodicities underlying the symbolic sequence are revealed as peaks at the respective frequencies in the spectrum plot.

The indicator sequences are obviously redundant, implying that their spectral counterparts are also redundant. Moreover, this redundancy can be expressed by means of the linear recursion involving the coefficients of the polynomial (4.3.1), which allows for the conclusion that only m consecutive spectral components need to be known to determine all the spectral components of the associated indicator sequence, where m is the number of times the associated symbol appears in the symbolic sequence. Furthermore, this dependence could also be used to check for and even to correct errors in a predicted DNA sequence.

Chapter 5

Integrate-and-Fire Converter Reconstruction

5.1 Introduction

This chapter differs from the previous in that reconstruction of signals is done using continuous timing information (assuming that all the data for reconstruction is present in this information). The idea is to avoid analog-to-digital conversion, hence traditional (Galois field) error control coding and real number coding are not used here. This provides a different perspective on signal reconstruction. The contribution of this chapter is the formulation of the continuous-time problem for the discrete-time framework. Hence, the continuous case is sketched and the discrete case is more thoroughly studied.

Spiking neuron circuits such as integrate-and-fire converters can be used as substitutes for analog-to-digital converters (ADCs) in applications where simpler analog equipment is traded off for more complex reconstruction at the receiver, where power dissipation and circuit size are not an issue [51]. In this manner, the signal is transformed into a spike train by means of very simple and low-power equipment at the encoder and the signal is reconstructed at the decoder by the cost of more complex equipment. This is very useful, for example, in remote sensing and implanted biomedical devices where device size and energy can be quite limited. In contrast, the time and cost of reconstructing the signals is not as crucial.

The integrate-and-fire converter model considered [23] is one where the bandlimited

signal $x \in L^2(\mathbb{R})$ is integrated until its value reaches a certain value θ_k, during time $[t_k, t_{k+1}]$. Then an action potential is created and the integration is reset to zero. More precisely,

$$\int_{t_k}^{t_{k+1}} x(t)dt = \theta_k, \qquad k \in \mathbb{Z}, \tag{5.1.1}$$

where the firing times $T = \{t_k\}_{k\in\mathbb{Z}}$ and the values $\Theta = \{\theta_k\}_{k\in\mathbb{Z}}$ are known. The idea is to obtain a stable reconstruction for x, solely from the knowledge of T and Θ. It is then important that T be a set of sampling for x.

Without loss of generality, consider x bandlimited such that $\text{supp}(\hat{x}) \in [-1/2, 1/2]$. Recall that $\text{supp}(\hat{x}) = \{\omega : \hat{x}(\omega) \neq 0\}$. Then $\text{supp}(\hat{x}) \in [-1/2, 1/2]$, i.e.,

$$x(t) = \int_{-1/2}^{1/2} \hat{x}(\omega) e^{j2\pi\omega t} d\omega$$

means that the highest frequency of x is 0.5 Hz. Hence x can be retrieved by its samples at the Nyquist rate of 1 Hz. If T is such that $\inf_{n\neq m} |t_n - t_m| > 0$, then T is said to be separated. In turn, if T can be expressed as a disjoint union of a finite number of separated sequences, then T is said to be relatively separated [25] . Moreover, if

$$D^-(T) = \lim_{r\to\infty} \frac{n^-(r)}{r} > 1,$$

where $n^-(r)$ is the smallest number of elements of T inside any interval of length r, then it can be shown that T is a set of sampling for x [8, 24].

5.2 Iterative Reconstruction

Let T be relatively separated and such that $D^-(T) > 1$. Then T is a set of sampling for x. For reconstruction to be possible, it is necessary that x be the only bandlimited function ($\text{supp}(\hat{x}) \in [-1/2, 1/2]$) that satisfies (5.1.1). The following results were presented in [23].

5.2.1 Uniqueness

Assume that there exists $y \in L^2(\mathbb{R})$ such that $\text{supp}(\hat{y}) \in [-1/2, 1/2]$ and that satisfies (5.1.1), i.e.

$$\int_{t_k}^{t_{k+1}} y(t)dt = \theta_k, \qquad k \in \mathbb{Z}.$$

Let $z = x - y$. Then $\text{supp}(\hat{z}) \in [-1/2, 1/2]$ and

$$\begin{aligned} \int_{t_k}^{t_{k+1}} z(t)dt &= \int_{t_k}^{t_{k+1}} (x(t) - y(t))\, dt \\ &= \theta_k - \theta_k \\ &= 0, \qquad k \in \mathbb{Z}. \end{aligned}$$

From the continuity of z, it follows that there exist $t'_k \in [t_k, t_{k+1}]$ such that $z(t'_k) = 0$, for each $k \in \mathbb{Z}$. Then, by construction, $T' = \{t'_k\}_{k\in\mathbb{Z}}$ is relatively separated (details in [23]) and $D^-(T') = D^-(T) > 1$. Hence T' is a set of sampling for z and, therefore, $z = 0$. It follows that $x = y$, which proves the uniqueness of x. In other words, T and Θ fully determine the bandlimited function x.

5.2.2 The Area Operator

However, (5.1.1) may be satisfied by functions $y \in L^2(\mathbb{R})$ such that $\text{supp}(\hat{y}) \notin [-1/2, 1/2]$. In fact, it is possible to define an operator $C : L^2(\mathbb{R}) \to L^2(\mathbb{R})$ such that $\text{Im}\, C$ is the set of functions in $L^2(\mathbb{R})$ satisfying (5.1.1). More precisely, for any $y \in L^2(\mathbb{R})$, $z = Cy$ satisfies

$$\int_{t_k}^{t_{k+1}} z(t)dt = \theta_k, \qquad k \in \mathbb{Z}.$$

Then C can be chosen to be

$$z(t) = y(t) + \frac{\theta_k}{t_{k+1} - t_k} - \frac{1}{t_{k+1} - t_k} \int_{t_k}^{t_{k+1}} y(t)dt, \quad t \in (t_k, t_{k+1}). \tag{5.2.1}$$

This means that C adjusts the area of y in each interval $[t_k, t_{k+1}]$ to θ_k ($k \in \mathbb{Z}$). Hence, C is named the area operator. If y already satisfies (5.1.1) or equivalently $y \in \operatorname{Im} C$, then $Cy = y$. This is the same as saying that C is a projection. Then for the bandlimited function x, it holds that $x = Cx$ or $x \in \operatorname{Im} C$.

But C has another special property. For $y \in L^2(\mathbb{R})$ fixed, Cy is actually the solution to the problem

$$\arg \min_{z \in \operatorname{Im} C} \|y - z\|.$$

To show this, consider the following problem.

Let $I = (a, b)$, $\theta \in \mathbb{R}$ and $f \in L^2(I)$. Consider the minimization problem

$$\arg \min_{g \in L^2(I)} \|f - g\|$$

where g must satisfy

$$\int_a^b g(t)dt = \theta.$$

Then the Lagrangian of this problem is given by $L(f, g) = (f - g)^2 - \lambda g$ which does not depend on g'. The Euler-Lagrange equations

$$\frac{\partial L}{\partial g} - \frac{d}{dt}\frac{\partial L}{\partial g'} = 0$$

become

$$-2(f - g) + \lambda = 0$$

or equivalently

$$g = f - \frac{\lambda}{2}.$$

It follows that

$$\theta = \int_I g(t)dt = \int_I (f(t) - \lambda/2)dt$$

which yields

$$\lambda = -\frac{2\theta}{b-a} + \frac{2}{b-a}\int_I f(t)dt.$$

Then g is given by

$$g(t) = f(t) + \frac{\theta}{b-a} - \frac{1}{b-a}\int_a^b f(t)dt, \quad t \in (a,b). \tag{5.2.2}$$

Note that (5.2.2) coincides with (5.2.1) in each interval (t_k, t_{k+1}). Since the $L^2(\mathbb{R})$ norm can be expressed by the sum of the norms over each interval,

$$\begin{aligned} \|y-z\|^2 &= \int_{\mathbb{R}} (y(t)-z(t))^2 dt \\ &= \sum_{k\in\mathbb{Z}} \int_{t_k}^{t_{k+1}} (y(t)-z(t))^2 dt, \end{aligned}$$

then Cy is, in fact, the closest function in $\operatorname{Im} C$ to y in the L^2 norm sense.

5.2.3 Iterative Method

Let B be the bandlimiting operator such that for any $y \in L^2(\mathbb{R})$, $\operatorname{supp}(\widehat{By}) \in [-1/2, 1/2]$. Then for the bandlimited function x, it holds that $x \in \operatorname{Im} B$. In fact, for any $y \in L^2(\mathbb{R})$ such that $\operatorname{supp}(\hat{y}) \in [-1/2, 1/2]$, $y \in \operatorname{Im} B$. Hence B is a projection. Moreover, $\operatorname{Im} B$ is a linear subspace of $L^2(\mathbb{R})$ and, therefore, B is a projection onto the convex set $\operatorname{Im} B$.

In turn, for $y, z \in \operatorname{Im} C$ and $\alpha \in [0,1]$,

$$\begin{aligned} \int_{t_k}^{t_{k+1}} [\alpha y(t) - (1-\alpha)z(t)]\, dt &= \alpha \int_{t_k}^{t_{k+1}} y(t)dt + (1-\alpha)\int_{t_k}^{t_{k+1}} z(t)dt \\ &= \alpha\theta_k + (1-\alpha)\theta_k \\ &= \theta_k, \qquad k \in \mathbb{Z}. \end{aligned}$$

Then $\alpha y + (1-\alpha)z \in \operatorname{Im} C$. Thus C is a projection onto the convex set $\operatorname{Im} C$.

Recall that x is the only function such that $\text{supp}(\hat{x}) \in [-1/2, 1/2]$ which belongs to $\text{Im}\, C$ and, therefore, $\text{Im}\, C \cap \text{Im}\, B = \{x\}$. In these conditions, the iterative method

$$y^{(k+1)} = BCy^{(k)} \tag{5.2.3}$$

with $y^{(0)} \in L^2(\mathbb{R})$ arbitrary, is a sequence of alternating projections (POCS) which converges to x. Then (5.2.3) is an iterative reconstruction procedure for x, motivated by fact that x must be bandlimited and that T and Θ fully characterize x.

5.3 The Discrete Framework

Sometimes, in practice, only a finite number of samples of the continuous signal is available, and not the signal itself. In this case, the signal made available is a vector $x \in \mathbb{R}^N$. Hence, the discrete-time finite-dimensional version of the problem considered so far is addressed. To apply the integrate-and-fire converter model, the discrete representation of x at instants $T = \{t_1, ..., t_n\}$ is given by

$$\sum_{i=t_k}^{t_{k+1}-1} x_i = \theta_k, \tag{5.3.1}$$

where $\Theta = \{\theta_1, ..., \theta_{n-1}\} \subset \mathbb{R}$ and $1 = t_1 < t_2 < ... < t_n = N$.

Again x must be bandlimited which can be traduced, in this context, by the existence of a matrix B of order N with $2m + 1$ nonzero spectral components such that $x = Bx$ (with $0 < 2m + 1 < n - 1$). Then B is a projection onto a $2m + 1$ dimensional subspace of $\mathbb{R}^N$. Once more it is desired that x be fully determined by T and Θ.

5.3.1 Uniqueness

Analogously as done for the continuous case, assume that there exists $y \in \mathbb{R}^N$, distinct from x, such that $y = By$ and y satisfies (5.3.1).

Let $z = x - y$. Then $z = Bz$ and

$$\sum_{i=t_k}^{t_{k+1}-1} z_i \quad = \quad \sum_{i=t_k}^{t_{k+1}-1} (x_i - y_i)$$

$$\begin{aligned} &= \theta_k - \theta_k \\ &= 0, \qquad k = 1, ..., n-1. \end{aligned} \tag{5.3.2}$$

Since $z = Bz$ and B has $2m+1$ nonzero spectral components, then it is possible to write z_k, $k = 1, ..., N$, as

$$z_k = \sum_{p=-m}^{m} \hat{z}_p \, e^{j2\pi pk/N}$$

which can in turn be written as

$$z_k = \sum_{p=-m}^{m} \hat{z}_p \, e^{j2\pi pw}$$

where $w = k/N$. Note that

$$P(w) = \sum_{p=-m}^{m} \hat{z}_p \, e^{j2\pi pw}$$

is a polynomial in w and, hence, $z_k = P(k/N)$.

$P(w)$ is a real polynomial in $e^{j2\pi w}$ of degree $\leq 2m+1$. Suppose that $P(w) \not\equiv 0$, i.e., $P(w)$ is not identically zero. By (5.3.2), $P(w)$ changes sign at least $n-1$ times. This means that because $P(w)$ is real and continuous, $P(w)$ has at least $n-1$ zeros. But $P(w)$ has degree $\leq 2m+1$ and $P(w) \not\equiv 0$ which implies that $P(w)$ has at most $2m+1 < n-1$ zeros, which contradicts the above condition. Then $P(w) \equiv 0$ which implies that $z_i = 0$ for $i = 1, ..., N$ and so $z = 0$, which contradicts the hypothesis that x and y are distinct. It follows that $x = y$ and, therefore, the bandlimited vector x is unique. Hence, T and Θ characterize x.

5.3.2 Adjusting Operator

In the continuous case, C was named the area operator since it adjusted the area of $y \in L^2(\mathbb{R})$ to satisfy (5.1.1). Its discrete counterpart, $C : \mathbb{R}^N \to \mathbb{R}^N$, adjusts the sum of the components (and not the area) of any $y \in \mathbb{R}^N$ to satisfy (5.3.1). Hence, in this case, C

will be simply called the adjusting operator. Formally, for any $y \in \mathbb{R}^N$, $z = Cy$ verifies

$$\sum_{i=t_k}^{t_{k+1}-1} z_i = \theta_k, \quad k = 1, .., n-1.$$

Then one choice for C is

$$z_p = y_p + \frac{\theta_k}{t_{k+1} - t_k} - \frac{1}{t_{k+1} - t_k} \sum_{i=t_k}^{t_{k+1}-1} y_i, \quad p \in \{t_k, ..., t_{k+1}\}.$$

The adjusting operator C is also a projection and, therefore, the bandlimited vector x satisfies $x = Cx$.

5.3.3 Iterative Reconstruction

Since x is the only vector that simultaneously verifies $x = Bx$ and $x = Cx$, it holds that $\operatorname{Im} B \cap \operatorname{Im} C = \{x\}$. Following the line of thought for the continuous case, $\operatorname{Im} B$ and $\operatorname{Im} C$ are convex sets and, hence, B and C are projections onto convex sets (POCS). Therefore,

$$y^{(k+1)} = BCy^{(k)} \tag{5.3.3}$$

with $y^{(0)} \in \mathbb{R}^N$, converges to x. Then (5.3.3) is an iterative procedure to reconstruct the discrete signal x.

5.4 Conclusion

The integrate-and-fire converter model was presented for the continuous ($L^2(\mathbb{R})$) and discrete ($\mathbb{R}^N$) cases. The differences contain some subtle details and while (5.1.1) can be traduced as an area, (5.3.1) cannot. This is why the operator C is named the area operator for $L^2(\mathbb{R})$ and the adjusting operator for $\mathbb{R}^N$.

Note that for the continuous case, the uniqueness of x is guaranteed by the fact that T is relatively separated and $D^-(T) > 1$, a sufficient condition for T to be a set of sampling. However, the discrete case does not require such subtleness. In fact, it suffices to have $2m + 1 < n - 1$ to guarantee the uniqueness of x.

The iterative methods presented for both cases are the continuous and discrete counterparts of an alternating POCS sequence and, thus, the convergence is guaranteed by the uniqueness of x. It constitutes, therefore, an iterative procedure to reconstruct the signal x in a stable manner.

Chapter 6

Conclusion

In the framework of DFT codes, discussed in Chapter 2, the problem of locating errors can be solved by applying the error-locating polynomial given by (2.2.5). This is a nonlinear problem. Formally, the unknown positions of lost samples $\{i_0, ..., i_{n-1}\}$ can be determined by taking n to be the maximum number of errors that is possible to be located and calculating the coefficients $\{h_k\}_{k=1}^{n}$. Then it is possible to determine the roots of $P(e^{-i2\pi i_p/N})$, $p = 0, ..., n-1$ and, hence, know $\{i_0, ..., i_{n-1}\}$.

Once the detection is solved, the errors become erasures. Now the problem is one of erasure recovery, which is a linear problem. The samples can be reconstructed by using information from the remaining samples (oversampling is required, this is, $K < N$), as long as the number of missing samples is less than K. This is achieved by (2.2.4), where B is actually a projection onto the code subspace and D is the matrix of the positions of known samples.

Although DFT codes are efficient for recovering missing data in dispersed patterns, they are highly unstable for bursty losses. To overcome such a problem, permutation of samples in order to scatter contiguous patterns is used. However, because there are certain patterns that the interleaver maps into a bursty fashion, two channels are employed where only one of the channels uses an interleaver, as depicted in Figure 2.2. Hence, it may always be possible, in general, to find a dispersed pattern for at least one of the channels.

The two-channel codes perform far better, especially for bursty erasure patterns. Indeed Figure 2.5 confirms the discrepancy between the conditioning of both codes, for contiguous

losses. The interleaver adds randomness to the code and it is this randomness that is responsible for the good performance of the code. Further discussion into how the interleaver intervenes is deserved and a formal mathematical demonstration has not yet been established. In fact, it is not yet known how to characterize the "best" permutations or the "worst" non-trivial ones. To add even more randomness, random gaussian codes were considered and indeed were shown to have exceptional performance, as confirmed by Figure 2.5. Moreover, it is possible to detect errors with these matrices, even though they have no specific structure. Under sparsity conditions, the detection can be solved as a linear programming problem. The correction of errors with real random block codes is one of the contributions of this thesis [48].

In the context of two-channel sampling and similarly to the single channel case, recovery of lost data requires redundancy so that there is enough information in the remaining samples to allow for reconstruction. Therefore, oversampling plays an important role in avoiding retransmission of the signal and further delays. In this context, oversampled series expansions can also be employed for reconstruction. A particular case is the function and derivative oversampled filter bank (multichannel sampling), where the two-channel structure is studied in Chapter 3. The oversampled series expansion was established and simplified into (3.4.2).

When the oversampling parameter is $r < 1/2$, each of the channels is oversampled and, thus, each channel alone can recover the lost samples: this is reduced to the classical sampling situation where any finite number of lost samples can be reconstructed. However, when $1/2 \leq r < 1$ the channels alone are incapable of reconstruction in the presence of erasures, although the filter-bank is oversampled. Hence, to reconstruct the signal, information from both channels must be taken into consideration. To our knowledge, this situation had not been studied before and, hence, is another contribution of the thesis [40, 41, 42].

The recovery of lost samples was divided into three cases: i) only missing function samples, ii) only missing derivative samples and iii) function and derivative samples missing simultaneously. For the first two cases, reconstruction is possible since the matrices involved

($I-S_1$ and $I-S_2'$) are always invertible. Nevertheless, the third case revealed more delicate. In fact, reconstruction is not always possible and simple sufficient conditions were provided for reconstruction. It remains to characterize the invertibility of the system matrix S and, hence, characterize the situations for which reconstruction is possible.

The two-channel structure with both function and derivative losses is very unstable (in contrast to the two-channel DFT codes) as confirmed by Figure 3.7, even for random erasure patterns. Even when $r \ll 1$ the system may be very unstable as shown in Figure 3.8. In this figure, there is great instability for $r_1 = 0.596$ in contrast to $r_2 = 0.616$ where the stability is much better although r_2 is closer to unity than r_1. This is made evident in Figure 3.9. Further study into the invertibility and conditioning of S is required.

Generalizations of the above results to filter banks with two arbitrary channels were presented in [26] and follow the line of thought of [40, 41]. Curiously, the reconstruction of the bandlimited signal may not be guaranteed even if the missing samples belong all to the same channel. Reconstruction, in this case, depends strongly on the analysis filters, h_1 and h_2. This impossibility of reconstruction in the two-channel case is very surprising, bearing in mind the corresponding and well known results in the classical (single channel) case, and are among the most intriguing results uncovered in the thesis.

The case for which the condition $|\det a(w)| \geq \alpha$ is relaxed for an interval $[-\delta, 0]$, where $\delta > 0$ is small, is presently being studied. For a signal f such that $\hat{f}(w) = 0$ in $w \in [-\delta, \delta]$, reconstruction seems possible since the results are apparently applicable outside the interval $[-\delta, \delta]$.

In Chapter 4 and returning to the error-locating polynomial discussed in Chapter 2, an interesting application to DNA sequences was found. Obtaining indicator sequences for a DNA sequence is a common procedure to transform symbolic sequences into numerical sequences. Because the alphabet associated to DNA sequences is $\{A, C, G, T\}$, for each DNA sequence one obtains four indicator sequences, i_A, i_C, i_G, i_T, as described in Section 4.2.

The spectral coefficients for these sequences are related by means of (4.4.1), where $\{h_k\}_{k=0}^{m-1}$ are the coefficients of the error-locating polynomial. This means that the coeffi-

cients are redundant and, hence, a set of n such coefficients can be determined by another set of m such coefficients. This dependency might motivate detection and correction of errors that can eventually occur in a given DNA indicator sequence. The fact that each of the four indicator sequences, in which a DNA sequence can be decomposed, can independently be predicted from a subset of its elements is yet another contribution [1, 2].

In Chapter 5, a rather different approach to reconstruction is presented: the integrate-and-fire model. The signal is reconstructed from a set of firing times T and from a set of threshold values Θ, where T and Θ are related by (5.1.1). This equation actually measures the area of the signal in the interval (t_k, t_{k+1}), with $t_k, t_{k+1} \in T$. The fact that these two sets determine the signal is guaranteed by the condition that the signal is bandlimited and that T is relatively separated and $D^-(T) > 1$. Then, taking into account that the bandlimiting operator and the area operator, given by (5.2.1), are projections onto convex sets, an iterative method exists that can stably recover the signal.

For discrete signals, the idea is very similar. Now T and Θ are related by (5.3.1) and the uniqueness of the signal is due to the fact that it is bandlimited and that $2m+1 < n-1$ (sufficient condition for T to be a set of sampling). The iterative method is analogous to the continuous case and, hence, it is possible to stably recover discrete signals too. This reconstruction technique is also a contribution of the thesis.

Future work includes the continued study of the interleaver in DFT codes, in hope to characterize "good" permutations. This may also undergo the mapping of the codes into graphs, if any insight into the problem can be achieved. Describing how the interleaver interferes exactly would be very important to understand the good performance of the two-channel structure. Also further work on random codes is being conducted. Moreover and relative to the function and derivative filter bank, study of the reconstruction when sample loss affects both channels deserves further attention. Situations when reconstruction is possible should be characterized and the stability better understood. More general conditions for invertible and stable conditions are also being pursued.

Appendix A

Function and Derivative Expansion

Consider Figure 3.2 where f is a finite-energy function bandlimited to ω_a Hz. The transfer matrix is given by

$$a(\omega) = \begin{pmatrix} 1 & i\omega \\ 1 & i\omega - i\omega_s \end{pmatrix}$$

where ω_s is the sampling frequency in each channel.

The projections of the impulses responses of the analysis filters (denoted by s_1 and s_2, respectively) satisfies the condition given by

$$\begin{pmatrix} 1 & i\omega \\ 1 & i\omega - i\omega_s \end{pmatrix} \begin{pmatrix} \hat{s}_1(\omega) \\ \hat{s}_2(\omega) \end{pmatrix} = \begin{pmatrix} \sqrt{2\pi}/\omega_s \\ 0 \end{pmatrix}, \quad \omega \in [0, \omega_a]$$

(an analogous condition exists for $\omega \in [-\omega_a, 0]$). Solving this equation (and that for negative values of ω) one obtains

$$\begin{aligned} \hat{s}_1(\omega) &= \frac{i\ \mathrm{sgn}(\omega)}{\sqrt{2\pi}} i\omega + \frac{\sqrt{2\pi}}{\omega_s}, \quad \omega \in [-\omega_a, \omega_a] \\ \hat{s}_2(\omega) &= \frac{-i\ \mathrm{sgn}(\omega)}{\sqrt{2\pi}}, \quad \omega \in [-\omega_a, \omega_a]. \end{aligned}$$

Hence, considering $\alpha = \omega_s/\sqrt{2\pi}$ it follows that

$$s_1(t) = \frac{1}{\sqrt{2\pi}} \int_{-\omega_a}^{\omega_a} \hat{s}_1(\omega) e^{i\omega t} d\omega$$

$$
\begin{aligned}
&= \frac{1}{\sqrt{2\pi}} \int_{-\omega_a}^{\omega_a} \left(\frac{i\,\mathrm{sgn}(\omega)}{\alpha\omega_s} i\omega + \frac{1}{\alpha} \right) e^{i\omega t} d\omega \\
&= \frac{1}{\sqrt{2\pi}} \int_{-\omega_a}^{\omega_a} \left(-\frac{\mathrm{sgn}(\omega)\omega}{\alpha\omega_s} + \frac{1}{\alpha} \right) e^{i\omega t} d\omega \\
&= \frac{1}{\sqrt{2\pi}} \int_{-\omega_a}^{0} \frac{\omega + \omega_s}{\alpha\omega_s} e^{i\omega t} d\omega + \frac{1}{\sqrt{2\pi}} \int_{0}^{\omega_a} \frac{-\omega + \omega_s}{\alpha\omega_s} e^{i\omega t} d\omega
\end{aligned}
$$

which leads to

$$
\begin{aligned}
s_1(t) &= -\frac{i\omega_a}{\omega_s^2 t} e^{-i\omega_a t} + \frac{i}{\omega_s t} e^{-i\omega_a t} - \frac{e^{-i\omega_a t}}{\omega_s^2 t^2} + \frac{2}{\omega_s^2 t^2} + \frac{i\omega_a}{\omega_s^2 t} e^{i\omega_a t} - \frac{i}{\omega_s t} e^{i\omega_a t} - \frac{e^{i\omega_a t}}{\omega_s^2 t^2} \\
&= -\frac{i\omega_a}{\omega_s^2 t} (\cos(-\omega_a t) + i \sin(-\omega_a t)) + \frac{i}{\omega_s t} (\cos(-\omega_a t) + i \sin(-\omega_a t)) - \\
&\quad \frac{1}{\omega_s^2 t^2} (\cos(-\omega_a t) + i \sin(-\omega_a t)) + \frac{2}{\omega_s^2 t^2} + \frac{i\omega_a}{\omega_s^2 t} (\cos(\omega_a t) + i \sin(\omega_a t)) - \\
&\quad \frac{i}{\omega_s t} (\cos(\omega_a t) + i \sin(\omega_a t)) - \frac{1}{\omega_s^2 t^2} (\cos(\omega_a t) + i \sin(\omega_a t)) \\
&= \frac{2i^2\omega_a}{\omega_s^2 t} \sin(\omega_a t) - \frac{2i^2}{\omega_s t} \sin(\omega_a t) - \frac{2}{\omega_s^2 t^2} \cos(-\omega_a t) + \frac{2}{\omega_s^2 t^2} \\
&= -\frac{2\omega_a}{\omega_s^2 t} \sin(\omega_a t) + \frac{2}{\omega_s t} \sin(\omega_a t) + \frac{2}{\omega_s^2 t^2} (1 - \cos(\omega_a t)) \\
&= 2\frac{-\omega_a + \omega_s}{\omega_s^2 t} \sin(\omega_a t) + \frac{2}{\omega_s^2 t^2} \left(1 - \cos^2\left(\frac{\omega_a t}{2}\right) + \sin^2\left(\frac{\omega_a t}{2}\right) \right) \\
&= 2\frac{-\omega_a + \omega_s}{\omega_s^2 t} \sin(\omega_a t) + \frac{2}{\omega_s^2 t^2} 2\sin^2\left(\frac{\omega_a t}{2}\right) \\
&= 2\omega_a \frac{-\omega_a + \omega_s}{\omega_s^2} \frac{\sin(\omega_a t\pi/\pi)}{\omega_a t\pi/\pi} + \frac{\omega_a^2}{\omega_s^2} \frac{\sin^2(\omega_a t\pi/2\pi)}{\omega_a t\pi/2\pi \;\; \omega_a t\pi/2\pi} \\
&= 2\left(\frac{\omega_a}{\omega_s} - \frac{\omega_a^2}{\omega_s^2}\right) \mathrm{sinc}\left(\frac{\omega_a t}{\pi}\right) + \frac{\omega_a^2}{\omega_s^2} \mathrm{sinc}^2\left(\frac{\omega_a t}{2\pi}\right).
\end{aligned}
$$

In the same way,

$$s_2(t) = \frac{1}{\sqrt{2\pi}} \int_0^{\omega_a} \frac{1}{\alpha i \omega_s} e^{i\omega t} d\omega - \frac{1}{\sqrt{2\pi}} \int_{-\omega_a}^{0} \frac{1}{\alpha i \omega_s} e^{i\omega t} d\omega$$

which leads to

$$\begin{aligned} s_2(t) &= -\frac{1}{\omega_s^2 t}(e^{i\omega_a t - 1}) + \frac{1}{\omega_s^2 t}(1 - e^{-i\omega_a t}) \\ &= \frac{1}{\omega_s^2 t}(2 - 2\cos(\omega_a t)) \\ &= \frac{\omega_a^2}{\omega_s^2} t \mathrm{sinc}^2\left(\frac{\omega_a t}{2\pi}\right). \end{aligned}$$

Considering the oversampling parameter $r = \omega_a/\omega_s$ and normalizing ω_s ($\omega_s = 1$), the above expressions simplify to

$$\begin{aligned} s_1(t) &= 2r(1-r)\mathrm{sinc}(2rt) + r^2\mathrm{sinc}^2(rt) \\ s_2(t) &= r^2 t \mathrm{sinc}^2(rt). \end{aligned}$$

Appendix B

Function and Delayed Derivative Expansion

Consider Figure 3.2 where f is a finite-energy function bandlimited to ω_a Hz. However, let there be a delay δ associated with the derivative samples. Then the transfer matrix is given by

$$a(\omega) = \begin{pmatrix} 1 & i\omega e^{-i\omega\delta} \\ 1 & i(\omega-\omega_s)e^{-i(\omega-\omega_s)\delta} \end{pmatrix}$$

where ω_s is the sampling frequency in each channel.

The projections of the impulses responses of the analysis filters (denoted by s_1 and s_2, respectively) satisfies the equations given by

$$\begin{pmatrix} 1 & i\omega e^{-i\omega\delta} \\ 1 & i(\omega-\omega_s)e^{-i(\omega-\omega_s)\delta} \end{pmatrix} \begin{pmatrix} \hat{s}_1(\omega) \\ \hat{s}_2(\omega) \end{pmatrix} = \begin{pmatrix} \sqrt{2\pi}/\omega_s \\ 0 \end{pmatrix}, \quad \omega \in [0, \omega_a]$$

$$\begin{pmatrix} 1 & i\omega e^{-i\omega\delta} \\ 1 & i(\omega+\omega_s)e^{-i(\omega+\omega_s)\delta} \end{pmatrix} \begin{pmatrix} \hat{s}_1(\omega) \\ \hat{s}_2(\omega) \end{pmatrix} = \begin{pmatrix} \sqrt{2\pi}/\omega_s \\ 0 \end{pmatrix}, \quad \omega \in [-\omega_a, 0].$$

B.1 Expression for s_1

Solving the system one obtains,

$$\hat{s}_1(\omega) = \frac{\sqrt{2\pi}}{\omega_s} \frac{\omega - \omega_s}{\omega - \omega_s - \omega e^{-i\delta\omega_s}}$$

$$= \frac{\sqrt{2\pi}}{\omega_s}\frac{\omega-\omega_s}{(1-e^{-i\delta\omega_s})\omega-\omega_s}, \quad \omega\in[0,\omega_a]$$

$$\hat{s}_1(\omega) = \frac{\sqrt{2\pi}}{\omega_s}\frac{\omega+\omega_s}{\omega+\omega_s-\omega e^{i\delta\omega_s}}$$

$$= \frac{\sqrt{2\pi}}{\omega_s}\frac{\omega+\omega_s}{(1-e^{i\delta\omega_s})\omega+\omega_s}, \quad \omega\in[-\omega_a,0].$$

Using the notations $a=1-e^{-i\delta\omega_s}$, $b=\omega_s$ and $c=1-e^{i\delta\omega_s}$, the above expressions simplify to

$$\hat{s}_1(\omega) = \frac{\sqrt{2\pi}}{b}\frac{b-\omega}{b-a\omega}$$

$$= \frac{\sqrt{2\pi}}{b}\frac{1-\omega/b}{1-a\omega/b}, \quad \omega\in[0,\omega_a]$$

$$\hat{s}_1(\omega) = \frac{\sqrt{2\pi}}{b}\frac{b+\omega}{b+c\omega}$$

$$= \frac{\sqrt{2\pi}}{b}\frac{1+\omega/b}{1+c\omega/b}, \quad \omega\in[-\omega_a,0].$$

Expanding the expressions yields

$$\hat{s}_1(\omega) = \frac{\sqrt{2\pi}}{b}\left(1+(a-1)\frac{\omega}{b}+a(a-1)\left(\frac{\omega}{b}\right)^2+a^2(a-1)\left(\frac{\omega}{b}\right)^3+...\right)$$

$$= \frac{\sqrt{2\pi}}{b}\left(1+\frac{a-1}{a}\sum_{n=1}^{\infty}\left(\frac{a\omega}{b}\right)^n\right), \quad \omega\in[0,\omega_a]$$

$$\hat{s}_1(\omega) = \frac{\sqrt{2\pi}}{b}\left(1-(c-1)\frac{\omega}{b}+c(c-1)\left(\frac{\omega}{b}\right)^2-c^2(c-1)\left(\frac{\omega}{b}\right)^3+...\right)$$

$$= \frac{\sqrt{2\pi}}{b}\left(1+\frac{c-1}{c}\sum_{n=1}^{\infty}\left(-\frac{c\omega}{b}\right)^n\right), \quad \omega\in[-\omega_a,0].$$

To have convergence for the geometric series, the conditions $|a\omega/b|<1$ and $|c\omega/b|<1$

must be verified. Then,

$$\left|\frac{a\omega}{b}\right| < 1$$

$$\left|\frac{(1-e^{-i\delta\omega_s})\omega}{\omega_s}\right| < 1$$

$$\frac{|(e^{i\delta\omega_s/2}-e^{-i\delta\omega_s/2})e^{-i\delta\omega_s}|\omega}{\omega_s} < 1$$

$$\frac{|\mathrm{cis}(\delta\omega_s/2)-\mathrm{cis}(-\delta\omega_s/2)|\omega}{\omega_s} < 1$$

$$|\sin(\delta\omega_s/2)|\frac{2\omega}{\omega_s} < 1$$

$$\omega\delta\frac{|\sin(\delta\omega_s/2)|}{\delta\omega_s/2} < 1, \quad \omega \in [0,\omega_a].$$

For $\omega_a < \omega_s = 2\pi$,

$$\omega\frac{|\sin(\pi\delta)|}{\pi} < 1$$

$$\omega|\sin(\pi\delta)| < \pi$$

$$\sin(\pi\delta) < \frac{\pi}{2\pi}$$

$$\pi\delta < \arcsin\left(\frac{1}{2}\right) = \frac{\pi}{6}$$

$$\delta < \frac{1}{6}.$$

The condition $|c\omega/b| < 1$ implies the same result.

So, for $\delta < 1/6$, s_1 exists and is given by

$$\begin{aligned} s_1(t) &= \frac{1}{\sqrt{2\pi}}\int_{-\omega_a}^{\omega_a}\hat{s}_1(\omega)e^{i\omega t}d\omega \\ &= \frac{1}{b}\int_{-\omega_a}^{0}e^{i\omega t}d\omega + \frac{1}{b}\frac{c-1}{c}\sum_{n=1}^{\infty}\left(-\frac{c}{b}\right)^n\int_{-\omega_a}^{0}\omega^n e^{i\omega t}d\omega + \end{aligned}$$

$$\frac{1}{b}\int_0^{\omega_a} e^{i\omega t}d\omega + \frac{1}{b}\frac{a-1}{a}\sum_{n=1}^{\infty}\left(\frac{a}{b}\right)^n \int_0^{\omega_a}\omega^n e^{i\omega t}d\omega.$$

Since

$$\frac{1}{\sqrt{2\pi}}\int_0^{\omega_a} e^{i\omega t}d\omega = \frac{it\omega_a^2}{2\sqrt{2\pi}}\mathrm{sinc}^2\left(\frac{\omega_a t}{2\pi}\right) + \frac{\omega_a}{\sqrt{2\pi}}\mathrm{sinc}\left(\frac{\omega_a t}{\pi}\right),$$

then

$$\frac{1}{\sqrt{2\pi}}\int_0^{\omega_a}\omega^n e^{i\omega t}d\omega = \frac{d^n}{dt^n}\left(\frac{it\omega_a^2}{2\sqrt{2\pi}}\mathrm{sinc}^2\left(\frac{\omega_a t}{2\pi}\right) + \frac{\omega_a}{\sqrt{2\pi}}\mathrm{sinc}\left(\frac{\omega_a t}{\pi}\right)\right).$$

If $e^{i\omega t}$ is also expanded,

$$e^{i\omega t} = \sum_{k=0}^{\infty}\frac{(it\omega)^k}{k!},$$

then

$$\begin{aligned} s_1(t) &= \frac{1}{b}\left(\frac{1}{it} - \frac{e^{-i\omega_a t}}{it}\right) + \frac{1}{b}\frac{c-1}{c}\sum_{n=1}^{\infty}\sum_{k=0}^{\infty}\left(-\frac{c}{b}\right)^n \frac{i^k t^k}{k!}\int_{-\omega_a}^{0}\omega^{n+k}d\omega + \\ &\quad \frac{1}{b}\left(\frac{e^{i\omega_a t}}{it} - \frac{1}{it}\right) + \frac{1}{b}\frac{a-1}{a}\sum_{n=1}^{\infty}\sum_{k=0}^{\infty}\left(\frac{a}{b}\right)^n \frac{i^k t^k}{k!}\int_0^{\omega_a}\omega^{n+k}d\omega \\ &= \frac{2}{bt}\sin(\omega_a t) - \frac{1}{b}\frac{c-1}{c}\sum_{n=1}^{\infty}\sum_{k=0}^{\infty}\left(-\frac{c}{b}\right)^n \frac{i^k t^k}{k!}\frac{(-\omega_a)^{n+k+1}}{n+k+1} + \\ &\quad \frac{1}{b}\frac{a-1}{a}\sum_{n=1}^{\infty}\sum_{k=0}^{\infty}\left(\frac{a}{b}\right)^n \frac{i^k t^k}{k!}\frac{\omega_a^{n+k+1}}{n+k+1}. \end{aligned}$$

However, it is possible to determine the expression of

$$\frac{d^n}{dt^n}\left(\frac{it\omega_a^2}{2\sqrt{2\pi}}\mathrm{sinc}^2\left(\frac{\omega_a t}{2\pi}\right) + \frac{\omega_a}{\sqrt{2\pi}}\mathrm{sinc}\left(\frac{\omega_a t}{\pi}\right)\right).$$

This yields

$$D(n,\omega_a) = \frac{d^n}{dt^n}\left(\frac{it\omega_a^2}{2\sqrt{2\pi}}\mathrm{sinc}^2\left(\frac{\omega_a t}{2\pi}\right) + \frac{\omega_a}{\sqrt{2\pi}}\mathrm{sinc}\left(\frac{\omega_a t}{\pi}\right)\right)$$

$$
\begin{aligned}
= \; & (-1)^n \frac{n!\sqrt{2}i\sin(\omega_a t/2)^2}{\sqrt{\pi}t^{n+1}} + (-1)^n \frac{n!}{2}\frac{\sqrt{2}\sin(\omega_a t)}{\sqrt{\pi}t^{n+1}} + \\
& \sum_{\substack{k=1 \\ k\,\text{odd}}}^{n} \left[(-1)^{n+1+(k-1)/2} \frac{\sqrt{2}i\, n!/k!\, \omega_a^k \sin(\omega_a t/2)\cos(\omega_a t/2)}{\sqrt{\pi}t^{n-k+1}} + \right. \\
& \left. (-1)^{n+1+(k-1)/2} \frac{\sqrt{2}n!}{2k!}\frac{\cos(\omega_a t)\omega_a^k}{\sqrt{\pi}t^{n-k+1}} \right] + \\
& \sum_{\substack{k=1 \\ k\,\text{even}}}^{n} \left[(-1)^{n+k/2-1} \frac{\sqrt{2}in!}{2k!}\frac{\cos(\omega_a t/2)^2\omega_a^k}{\sqrt{\pi}t^{n-k+1}} + (-1)^{n+k/2} \frac{\sqrt{2}in!}{2k!}\frac{\sin(\omega_a t/2)^2\omega_a^k}{\sqrt{\pi}t^{n-k+1}} + \right. \\
& \left. (-1)^{n+k/2} \frac{\sqrt{2}n!}{2k!}\frac{\sin(\omega_a t)\omega_a^k}{\sqrt{\pi}t^{n-k+1}} \right].
\end{aligned}
$$

Then,

$$
\begin{aligned}
s_1(t) \; = \; & -\frac{1}{b}D(0,-\omega_a) - \frac{1}{b}\frac{c-1}{c}\sum_{n=1}^{\infty}\left(-\frac{c}{b}\right)^n D(n,-\omega_a) + \\
& \frac{1}{b}D(0,\omega_a) + \frac{1}{b}\frac{a-1}{a}\sum_{n=1}^{\infty}\left(\frac{a}{b}\right)^n D(n,\omega_a).
\end{aligned}
$$

B.2 Expression for s_2

Analogously,

$$
\begin{aligned}
\hat{s}_2(\omega) \; &= \; -\frac{\sqrt{2\pi}}{\omega_s}\frac{1}{i(\omega-\omega_s)e^{-i\delta(\omega-\omega_s)} - i\omega e^{-i\delta\omega}}, \quad \omega \in [0,\omega_a], \\
\hat{s}_2(\omega) \; &= \; -\frac{\sqrt{2\pi}}{\omega_s}\frac{1}{i(\omega+\omega_s)e^{-i\delta(\omega+\omega_s)} - i\omega e^{-i\delta\omega}}, \quad \omega \in [-\omega_a,0].
\end{aligned}
$$

For $a = e^{-i\delta\omega_s}$, $b = \omega_s$ and $c = e^{i\delta\omega_s}$,

$$
\hat{s}_2(\omega) \; = \; \frac{\sqrt{2\pi}i}{b}\frac{1}{(\omega c - bc - \omega)e^{-i\delta\omega}}, \quad \omega \in [0,\omega_a],
$$

$$\hat{s}_2(\omega) = \frac{\sqrt{2\pi}i}{b}\frac{1}{(\omega a + ba - \omega)e^{-i\delta\omega}}, \quad \omega \in [-\omega_a, 0].$$

Expanding the expressions yields

$$\hat{s}_2(\omega) = -\frac{\sqrt{2\pi}i}{b}\sum_{n=0}^{\infty}\frac{(c-1)^n}{b^{n+1}c^{n+1}}\omega^n, \quad \omega \in [0, \omega_a],$$

$$\hat{s}_2(\omega) = \frac{\sqrt{2\pi}i}{b}\sum_{n=0}^{\infty}(-1)^n\frac{(a-1)^n}{b^{n+1}a^{n+1}}\omega^n, \quad \omega \in [-\omega_a, 0],$$

this is

$$\hat{s}_2(\omega) = -\frac{\sqrt{2\pi}i}{b^2c}\sum_{n=0}^{\infty}\frac{(c-1)^n}{b^nc^n}\omega^n, \quad \omega \in [0, \omega_a],$$

$$\hat{s}_2(\omega) = \frac{\sqrt{2\pi}i}{b^2a}\sum_{n=0}^{\infty}(-1)^n\frac{(a-1)^n}{b^na^n}\omega^n, \quad \omega \in [-\omega_a, 0].$$

Convergence occurs when

$$\left|\frac{c-1}{bc}\omega\right| < 1$$

and

$$\left|\frac{1-a}{ba}\omega\right| < 1.$$

For $\omega_s = 2\pi$ and $0 \leq \omega \leq \omega_a < 2\pi$, the first expression leads to

$$\left|\frac{e^{i\delta 2\pi} - 1}{2\pi e^{i\delta 2\pi}}\omega\right| < 1$$

$$\frac{\left|e^{i\delta 2\pi} - 1\right|\omega}{2\pi} < 1$$

$$|(e^{i\delta\pi} - e^{-i\delta\pi})e^{i\delta\pi}|\omega < 2\pi$$

$$|\mathrm{cis}(\delta\pi) - \mathrm{cis}(-\delta\pi)|\omega < 2\pi$$

$$2|\sin(\delta\pi)|\omega < 2\pi$$

$$|\sin(\delta\pi)| < \frac{\pi}{2\pi}$$

$$\delta\pi < \frac{\pi}{6}$$

$$\delta < \frac{1}{6}.$$

Similarly, the second expression leads to the same result.

It then follows that for $\delta < 1/6$, s_2 exists and is given by

$$\begin{aligned} s_2(t) &= \frac{i}{b}\sum_{n=0}^{\infty}(-1)^n\frac{(a-1)^n}{b^{n+1}a^{n+1}}\int_{-\omega_a}^{0}\omega^n e^{i\omega t}d\omega - \frac{i}{b}\sum_{n=0}^{\infty}\frac{(c-1)^n}{b^{n+1}c^{n+1}}\int_{0}^{\omega_a}\omega^n e^{i\omega t}d\omega \\ &= -\frac{i}{b}\sum_{n=0}^{\infty}(-1)^n\frac{(a-1)^n}{b^{n+1}a^{n+1}}D(n,-\omega_a) - \frac{i}{b}\sum_{n=0}^{\infty}\frac{(c-1)^n}{b^{n+1}c^{n+1}}D(n,\omega_a). \end{aligned}$$

Bibliography

[1] Afreixo, V.; Ferreira. P. J. S. G.; Santos, D. M. S.: Fourier Analysis of Symbolic Data: A Brief Review, *Digital Signal Processing* **14**, 523-530 (2004).

[2] Afreixo, V.; Ferreira. P. J. S. G.; Santos, D. M. S.: Spectrum and Symbol Distribution of Nucleotide Sequences, *Physical Review E* **70**, 031910 (2004).

[3] Anastassiou, D.: Genomic Signal Processing, *IEEE Signal Processing Magazine* **18**(4), 8-20 (2001).

[4] Berrou, C.; Glavieux, A.; Thitimajshima, P.: Near Shannon Limit Error-Correcting Coding and Decoding: Turbo-Codes, *Proceedings of the IEEE International Conference on Communications, ICC 93*, 1064-1070, Geneva (May 1993).

[5] Blahut, R. E.: *Algebraic Codes for Data Transmission*, Cambridge University Press, Cambridge, 2002.

[6] Boyd, S.; Vandenberghe, L.: *Convex Optimization*, Cambridge University Press, Cambridge, 2004.

[7] Brown, J. L. Jr.: Sampling of Bandlimited Signals: Fundamental Results and Some Extensions, *Handbook of Statistics* **10**, 59-101 (1993).

[8] Carleson, L.; Malliavin, P.; Neuberger, J.; Wermer, J.: *Collected Works of Arne Beurling. Volume 2, Harmonic Analysis*, Birkhäuser, Boston, 1989.

[9] Chen, Z.; Dongarra, J.: Numerically Stable Real-Number Codes Based on Random Matrices, *IEEE Information Theory Workshop 2004*, San Antonio, Texas, USA (October 2004).

[10] Chen, Z.; Dongarra, J.: Condition Numbers of Gaussian Random Matrices, *SIAM Journal on Matrix Analysis and Applications* **27**(3), 603-620 (2005).

[11] Chong, E. K. P.; Zak, S. H.: *An Introduction to Optimization*, John Wiley & Sons. Inc., USA, 1996.

[12] Conway, J. H.; Hardin, R. H.; Sloane, N. J. A.: Packing Lines, Planes, Etc.: Packings in Grassmannian Spaces, *Experimental Mathematics* **5**(2), 139-159 (1996).

[13] Donoho, D.; Huo, X.: Uncertainty Principles and Ideal Atomic Decomposition, *IEEE Transactions on Information Theory* **47**(7), 2845-2862 (2001).

[14] Donoho, D. L.; Elad, M.: Optimally Sparse Representation in General (Nonorthogonal), Dictionaries via ℓ^1 Minimization, *Proceedings of the National Academy of Sciences* **100**(5), 2197-2202 (2003).

[15] Elad, M.; Bruckstein, A. M.: A Generalized Uncertainty Principle and Sparse Representation in Pairs of Bases, *IEEE Transactions on Information Theory* **48**(9), 2558-2567 (2002).

[16] Ferreira, P. J. S. G.: Incomplete Sampling Series and the Recovery of Missing Samples from Oversampled Band-Limited Signals, *IEEE Trans. Signal Processing* **40**(1), 225-227 (January 1992).

[17] Ferreira, P. J. S. G.: The Stability of a Procedure for the Recovery of Lost Sampled in Band-Limited Signals, *Signal Processing* **40**(3), 195-205 (December 1994).

[18] Ferreira, P. J. S. G.: Sampling Series with an Infinite Number of Unknown Samples, *1995 International Workshop on Sampling Theory and Applications, SAMPTA 1995*, Jurmala, Latvia, September 1995.

[19] Ferreira, P. J. S. G.; Vieira, J. M. N.: Detection and Correction of Missing Samples, *Proceedings of the 1997 Workshop on Sampling Theory and Applications*, Aveiro, Portugal, 1997.

[20] Ferreira, P. J. S. G.: Mathematics for Multimedia Signal Processing II – Discrete Finite Frames and Signal Reconstruction, *Signal Processing for Multimedia*, 35-54 (1999).

[21] Ferreira, P. J. S. G.: Stability Issues in Error Control Coding in the Complex Field, Interpolation, and Frame Bounds, *IEEE Signal Processing Letters* **7**(3), 57-59 (March 2000).

[22] Ferreira, P. J. S. G.; Vieira, J. M. N.: Stable DFT Codes and Frames, *IEEE Signal Processing Letters* **10**(2), 50-53 (February 2003).

[23] Ferreira, P. J. S. G.: Reconstruction from the Output of an Integrate-and-Fire Converter, Internal Report 0504, IEETA, Aveiro University, 2005.

[24] Higgins, J. R.: *Sampling Theory in Fourier and Signal Analysis: Foundations*, Oxford University Press, Oxford, 1996.

[25] Jaffard, S.: A Density Criterion for Frames of Complex Exponentials, *Michigan Mathematical Journal* **38**(3), 339-348 (1991).

[26] Kim, J. M.; Kwon, K. H.: Recovery of Finite Missing Samples in Two-Channel Oversampling, *Sampling Theory in Signal and Image Processing* **6**(2), 185-198 (May 2007).

[27] Lee, W.; Luo, L.: Periodicity of Base Correlation in Nucleotide Sequence, *Physical Review E* **56**(1), 848-851 (1997).

[28] Malioutov, D. M.; Çetin, M.; Willsky, A. S.: Optimal Sparse Representations in General Overcomplete Bases, *Proceedings of the IEEE International Conference on Acoustics, Speech, and Signal Processing, ICASSP 2004* **II**, 793-796, Montreal, Canada (May 2004).

[29] Marshall, T. G. Jr.: Coding of Real-Number Sequences for Error Correction: a Digital Signal Processing Problem, *IEEE Journal on Selected Areas in Communications* **2**, 381-391 (March 1984).

[30] Marvasti, F. A., Nafie, M.: Sampling Theorem: A Unified Outlook on Information Theory, Block and Convolutional Codes, *IEICE Transactions on Fundamentals of Electronics, Communications and Computer Sciences* **E76-A**(9), 1383-1391 (September 1993).

[31] Marvasti, F. A. (Ed): *Nonuniform Sampling: Theory and Practice*, Kluwer Academic / Plenum Publishers, New York, 2001.

[32] Nair, V. S. S.; Abraham, J. A.: Real-Number Codes for Fault-Tolerant Matrix Operations on Processor Arrays, *IEEE Transactions on Computers* **39**(4), 426-435 (April 1990).

[33] Papoulis, A.; Generalized Sampling Expansion, *IEEE Transactions on Circuits and Systems* **24**(11), 652-654 (November 1977).

[34] Rath, G.; Guillemot, C.: Recursive syndrome decoding of DFT codes for bursty erasures, *Proceedings of the IEEE International Conference on Acoustics, Speech, and Signal Processing, ICASSP 2002* **3**, 2157-2160 (2002).

[35] Rath, G.; Guillemot, C.: Performance Analysis and Recursive Syndrome Decoding of DFT Codes for Bursty Erasure Recovery, *IEEE Transactions on Signal Processing* **51**(5), 1335-1350 (May 2003).

[36] Rath, G.; Guillemot, C.: Subspace Algorithms For Error Localization With DFT Codes, *Proceedings of the IEEE International Conference on Acoustics, Speech, and Signal Processing, ICASSP 2003* **IV**, 257-260, Hong-Kong (2003).

[37] Rath, G.; Guillemot, C.: Recent Advances in DFT Codes Based Quantized Frame Expansions for Erasure Channels, *Digital Signal Processing* **14**, 332-354 (2004).

[38] Rath, G.; Guillemot, C.: Frame-Theoretic Analysis of DFT Codes With Erasures, *IEEE Transactions on Signal Processing* **52**(2), 447-460 (February 2004).

[39] Rath, G.; Guillemot, C.: Subspace-Based Error and Erasure Correction with DFT Codes for Wireless Channels, *IEEE Transactions on Signal Processing* **52**(11), 3241-3252 (November 2004).

[40] Santos, D. M. S.; Ferreira, P. J. S. G.: Reconstruction from Missing Samples and Oversampled Filter Banks, *Proceedings of the IEEE International Conference on Acoustics, Speech, and Signal Processing, ICASSP 2004* **III**, 941-944, Montreal, Canada (May 2004).

[41] Santos, D. M. S.; Ferreira, P. J. S. G.; Vieira, J. M. N.: Study of the Recovery of Missing Samples for Function and Derivative Oversampled Filter Banks, *2005 International Workshop on Sampling Theory and Applications, SAMPTA 2005*, Samsun, Turkey (July 2005).

[42] Santos, D. M. S.; Ferreira, P. J. S. G.; Vieira, J. M. N.: Reconstruction from Function and Derivative Samples in the Presence of Erasures, submitted to *IEEE Transactions on Information Theory.*

[43] Shiu, J.; Wu, J. L.: Class of Majority Decodable Real-Number Codes, *IEEE Transactions on Communications* **44**(3), 281-283 (March 1996).

[44] Strohmer, T.; Heath, R. W. Jr.: Grassmannian Frames with Applications to Coding and Communication, *Applied and Computational Harmonic Analysis* **14**(3), 257-275 (2003).

[45] Vieira, J. M. N.; Ferreira, P. J. S. G.: Interpolation, Spectrum Analysis, Error-Control Coding, and Fault-Tolerant Computing, *Proceedings of the IEEE International Conference on Acoustics, Speech, and Signal Processing, ICASSP 97* **III**, 1831-1834, Munich, Germany (April 1997).

[46] Vieira, J. M. N.: *Reconstrução de Sinal e Codificação*, Ph.D. thesis, Departamento de Electrónica e Telecomunicações, Aveiro University, Aveiro, Portugal, 2000.

[47] Vieira, J. M. N.: Stability Analysis of Non-Recursive Parallel Concatenated Real Number Codes, *IEEE 2nd Signal Processing Education Workshop*, Pine Mountain, Georgia, USA (October 2002).

[48] Vieira, J. M. N.; Santos, D. M. S.; Ferreira, P. J. S. G.: Error Detection with Real-Number Codes Based on Random Matrices, *IEEE Digital Signal Processing Workshop, DSP Workshop 2006*, Wyoming, USA (September 2006).

[49] Vieira, M. S.: Statistics of DNA Sequences: A Low-Frequency Analysis, *Physical Review E* **60**(1), 5932-5937 (1999).

[50] Voss, R. F.: Evolution of Long-Range Fractal Correlations and $1/f$ Noise in DNA Base Sequences, *Physical Review Letters* **68**(25), 3805-3808 (1992).

[51] Wei, D.; Harris, J. G.: Signal Reconstruction from Spiking Neuron Models, *Proceedings of the 2004 International Symposium on Circuits and Systems, ISCAS'04* **V**, 353-356 (May 2004).

[52] Welch, L. R.: Lower Bounds on the Maximum Cross Correlation of Signals, *IEEE Transactions on Information Theory* **20**(3), 397-399 (1974).

[53] Wright, M. H.: The Interior-Point Revolution in Constrained Optimization, Technical Report 98-4-09, Bell Laboratories, 1998.